NASA TM X-172

TECHNICAL MEMORANDUM

X-172

AERODYNAMIC CHARACTERISTICS AT MACH NUMBERS OF 1.41 AND 2.01 OF A SERIES OF CRANKED WINGS RANGING IN ASPECT RATIO FROM 4.00 TO 1.74 IN COMBINATION WITH A BODY

By John R. Sevier, Jr.

Langley Research Center
Langley Field, Va.

Declassified February 6, 1962

NATIONAL AERONAUTICS AND SPACE ADMINISTRATION

WASHINGTON January 1960

NATIONAL AERONAUTICS AND SPACE ADMINISTRATION

TECHNICAL MEMORANDUM X-172

AERODYNAMIC CHARACTERISTICS AT MACH NUMBERS OF 1.41 AND 2.01 OF A SERIES OF CRANKED WINGS RANGING IN ASPECT RATIO FROM 4.00 TO 1.74 IN COMBINATION WITH A BODY

By John R. Sevier, Jr.

SUMMARY

A program has been conducted in the Langley 4- by 4-foot supersonic pressure tunnel to determine the effects of certain wing plan-form variations on the aerodynamic characteristics of wing-body combinations at supersonic speeds. The present report deals with the results of tests of a family of cranked wing plan forms in combination with an ogive-cylinder body of revolution. Tests were made at Mach numbers of 1.41 and 2.01 at corresponding values of Reynolds number per foot of 3.0×10^6 and 2.5×10^6.

Results of the tests indicate that the best overall characteristics were obtained with the low-aspect-ratio wings. Plan-form changes which involved decreasing the aspect ratio resulted in higher values of maximum lift-drag ratio, in addition to large increases in wing volume. Indications are that this trend would have continued to exist at aspect ratios even lower than the lowest considered in the present tests. Increases in the maximum lift-drag ratio of about 15 percent over the basic wing were achieved with practically no increase in drag.

The severe longitudinal stability associated with the basic cranked wing was no longer present (within the limits of the present tests) on the wings of lower aspect ratio formed by sweeping forward the inboard portion of the trailing edge.

INTRODUCTION

The selection of the wing plan form is one of the major decisions facing the aircraft designer. A good wing plan form should have low drag, high aerodynamic efficiency, and should provide a maximum of volume for fuel stowage. At the same time, it must have good structural characteristics and be so designed as not to result in poor stability characteristics. Of course, the final selection of the plan form will be a compromise between these requirements and will depend on their relative importance in a particular application. The present report presents the results of one phase of a plan-form program which was undertaken in the Langley 4- by 4-foot supersonic pressure tunnel to investigate the longitudinal stability characteristics of a series of plan forms with particular interest in evaluating their relative aerodynamic efficiencies.

From the standpoint of high aerodynamic efficiency at supersonic speeds, the highly swept wing is generally superior to other types of wings of comparable thickness ratios. However, one of the greatest disadvantages of the highly swept plan form has been the severe pitchup characteristic which is inherently associated with this plan form, especially in the transonic and low supersonic speed range. Occurring at lift coefficients low enough to be in the range of routine maneuvers, this instability cannot be eliminated by the usual "fixes" such as fences, leading-edge chord-extensions, boundary-layer ramps, and so forth, as demonstrated in the limited tests of reference 1. For this reason, then, the highly swept wing has met with little acceptance in current aircraft design.

One of the ideas advanced to alleviate the difficulty of pitchup has been the cranked wing. The cranked wing retains much of the efficiency of the conventional highly swept wing yet has the advantage that the loss in lift in the tip region (which causes pitchup) is less likely to occur due to the fact that the outboard portion of the wing is only moderately swept. In practice, however, the cranked wing is usually not successful in eliminating pitchup entirely but does succeed in postponing the instability to a somewhat higher lift coefficient than for the conventional highly swept wing.

The present report compares a conventional 60° swept wing with a cranked wing swept 60° inboard and 30° outboard and deals with several plan-form variations (based on work done in refs. 2 and 3) of the basic cranked wing designed to evaluate the relative merits of plan-form variation on aerodynamic efficiency and on the pitchup problem. Tests were made of the various wings in combination with an ogive-cylinder body of revolution at Mach numbers of 1.41 and 2.01 at corresponding Reynolds numbers per foot of 3.0×10^6 and 2.5×10^6. The plan-form variations

covered a wide range of aspect ratio (4.00 to 1.74) and taper ratio (0.33 to 0.09). Thickness ratio of the basic cranked wing was 0.06 and was constant along the span. The spanwise variation in absolute thickness remained the same for all the wings tested.

SYMBOLS

b	wing span
c	airfoil chord
c_r	airfoil chord at wing root (body center line)
$\bar{c}$	mean aerodynamic chord, $\dfrac{\int_0^{b/2} c^2\,dy}{\int_0^{b/2} c\,dy}$
C_D	drag coefficient based on area of respective wing, D/qS
$C_{D,min}$	minimum value of C_D
$C_{D,b}$	drag coefficient based on area of basic wing, D/qS_b
$(C_{D,b})_{min}$	minimum value of $C_{D,b}$
C_L	lift coefficient based on respective wing area, L/qS
$C_{L,b}$	lift coefficient based on basic wing area, L/qS_b
C_{L_α}	lift-curve slope of respective wings, $dC_L/d\alpha$, per degree; measured over linear portion of lift curve
$C_{L_\alpha,b}$	lift-curve slope of basic wing, $dC_{L,b}/d\alpha$, per degree; measured over linear portion of lift curve
C_m	pitching-moment coefficient, $m/qS\bar{c}$
D	drag

L	lift
m	pitching moment about the assumed center-of-gravity location (fig. 1(b))
M	free-stream Mach number
q	free-stream dynamic pressure
S	wing area including that portion blanketed by fuselage
S_b	area of basic cranked wing including that portion blanketed by fuselage
y	spanwise distance measured perpendicular to plane of symmetry

APPARATUS

Tunnel

All tests were conducted in the Langley 4- by 4-foot supersonic pressure tunnel which is a rectangular, closed-throat, single-return wind tunnel designed for a Mach number range of 1.2 to 2.2. The test section Mach number is varied by deflecting horizontal flexible walls against a series of fixed interchangeable templates which have been designed to produce uniform flow in the test section. For the present investigation, the test section Mach numbers were 1.41 and 2.01; the test section heights were 4.44 feet and 5.10 feet, respectively; and the test section width was 4.5 feet.

Models

Wings.- The wings were constructed as indicated in figures 1 and 2. Onto a steel spar, there could be attached a combination of forward and rearward inserts. In addition to the inserts which made up the basic 60° (inboard sweep)-30° (outboard sweep) swept wing, there were inserts which provided an increase of 67 percent to the basic center-line chord in the forward direction, and increases of 67, 133, and 200 percent in the rearward direction. For one series of inserts, the extension to the basic wing tapered linearly to zero at the 50-percent-semispan station (fig. 1(a)), while on the other series (fig. 1(b)), the extension tapered linearly to zero at the 70-percent-semispan station.

Photographs of representative wings are shown in figure 2. In order to identify the various configurations, a two unit numbering system,

with subscripts associated with each unit, has been adopted. The first number in the designation (0 or 67) refers to the leading-edge modification and designates the percentage by which the length of the center-line chord of the basic wing has been increased by the forward insert. The associated subscript refers to the spanwise extent (in percent semispan) of the leading-edge modification. Similarly, trailing-edge modifications are denoted by the second number of the designation (0, 67, 133, or 200) which refers to the percentage by which the center-line chord of the basic wing is increased by the rearward insert. As before, the subscript (50 or 70) refers to the spanwise extent (in percent semispan) of the modification. For example, the configuration designated 67_{50}-200_{70} (fig. 2(b)) refers to the wing on which the leading edge has been modified by increasing the center-line chord of the basic wing by 67 percent in the forward direction and tapering the chord increase linearly to zero at the 50-percent-semispan station; similarly, the trailing edge of the basic cranked wing has been modified by increasing the basic center-line chord by 200 percent in the rearward direction and tapering this modification linearly to zero at the 70-percent-semispan station.

In the case where a number in the designation is variable, that number will be replaced with an X. For example, when data from the family of wings with the basic leading edge are plotted as a function of trailing-edge extensions extending to the 50-percent semispan, the designation will be $0\text{-}X_{50}$.

As shown in figure 3, the airfoil section for the forward 1/3 chord of the basic wing was made up of the forward 1/3 of an NACA 63-006 airfoil section and was combined with a slab for the remaining 2/3 chord, resulting in a blunt trailing edge with a thickness equal to the maximum thickness of the airfoil at that particular spanwise station. It was necessary to modify the 63-series thickness distribution slightly near the 1/3-chord station in order to fair it in smoothly with the slab. For the wings with extensions, a leading edge identical to the basic wing was used and was combined with a slab having a length dependent upon the amount of extension.

The basic wing had a constant thickness ratio of 0.06. For the wings with extensions, the thickness ratio varied from one wing to the next depending on the amount of extension; however, on all the wings, the spanwise variation in absolute thickness remained the same as on the basic wing.

The wings were designed in the above manner so as to make possible a wide range of plan forms without causing the construction effort to become prohibitively large. Although the airfoil section used was not particularly good from the standpoint of aerodynamic efficiency, it was considered

adequate to fulfill the aim of this investigation, which was to evaluate the relative merits of wings with various plan forms but with the same variation in absolute thickness.

Sketches of the configuration tested along with pertinent geometric characteristics are presented in figure 4.

Fuselage.- An ogive-cylinder fuselage was tested in combination with the above-described wings mounted in the midposition (fig. 1). The fineness ratio of the ogive was 3.5.

A three-component internal strain-gage balance was housed within the fuselage for the purpose of measuring normal force, chord force, and pitching moment. Angle of attack was measured optically during the tests by means of a prism mounted on the fuselage.

TESTS

Tests were conducted at Mach numbers of 1.41 and 2.01 at corresponding Reynolds numbers per foot of 3.0×10^6 and 2.5×10^6, respectively. Tunnel stagnation pressure was 10 pounds per square inch absolute and stagnation temperature was 100° F. The tunnel dewpoint was maintained at a sufficiently low value to eliminate significant condensation effects.

In order to reduce the amount by which the base pressure needed to be adjusted to correspond to free-stream static pressure, a base plug was installed for all tests (fig. 1). The plug was concentric with the model base and was equal to the base diameter. A gap of approximately 1/16 inch separated the model base and the plug.

All data presented herein are for natural transition on the wing and body.

RESULTS AND DISCUSSION

General Remarks

As mentioned previously, all the wings had the same spanwise variation in absolute thickness. Such a design was considered to be more reasonable than one in which the thickness ratio t/c was constant for all wings, since if some compromise value of t/c had been selected and held constant for all wings, it would have resulted in an unrealistically low t/c for the high-aspect-ratio wings and an unrealistically high

t/c for the low-aspect-ratio wings. In actual practice, the design considerations involved in selecting the wing thickness would be a complex set of compromises involving volume required, bending moment, type of structure, flutter characteristics, etc.

Although the thickness ratio varied from one wing to the next, the streamwise section ahead of the slab remained the same for all wings, (fig. 3). Thus, wings with the same leading-edge configuration had about the same thickness drag. The 67_{50} leading-edge configuration had a somewhat lower thickness drag (over the inboard 50-percent semispan) than the 0 leading-edge configuration as a result of its thinner sections normal to the leading edge. In addition, as a result of the slab section the various wings had a base drag which varied in a manner dependent upon how the base pressure was affected by the boundary layer on the wing. No attempt was made in the present tests to estimate this effect.

Presentation of Results

A comparison is made in figure 5 of the basic wing-body combinations having the 60° swept and the 60°-30° cranked wings which are identical except in plan form. In figures 6 to 9 are presented the results from the series of cranked wing-body combinations, and in figure 10 the body-alone characteristics are presented. It should be noted that the reference areas and lengths used to nondimensionalize the forces and moments for the various wing-body combinations are those associated with each wing. The reference axis for the pitching moments, however, is a common one for all wings.

Plots of the basic data for the various cranked wing-body combinations tested are presented in figures 6 to 9. The most pertinent results from these data have been plotted as a function of trailing-edge extension in figures 11 to 15, and it is these summary plots which will primarily be the subject of the present discussion. In discussing the relative merits of the various wing plan forms it should be kept in mind that the differences in areas (from one plan form to another) used to nondimensionalize the forces can cause changes in the coefficients which are not necessarily reflected in the forces themselves. For example, as extensions are added to the basic wing, the drag coefficient is reduced but in most cases the actual drag force is increased. For this reason, then, plots of minimum drag coefficients, lift-curve slope, and drag-due-to-lift parameter are presented (figs. 11 to 13) in which the coefficients are based both on the respective wing areas and on the area of the basic wing. The latter method then permits a valid comparison of actual force variations between the different wings since the coefficients for all the wings are based on a common area.

Basic Wings

The comparison of the conventional swept wing and the cranked wing in figure 5 shows the cranked wing to have a somewhat lower value of $(L/D)_{max}$ occurring at a higher C_L. In addition, the cranked configuration will have a somewhat higher drag than the swept configuration when both are operating (with the same wing loading) at the appropriate altitudes to fly at C_L for $(L/D)_{max}$. It should be noted that although pitchup does occur at a higher lift coefficient than $(L/D)_{max}$ the margin of safety might not be considered sufficient to allow operation of either configuration at $(L/D)_{max}$.

Stability

Examination of figure 5 shows the severe pitchup characteristics of the basic 60° swept wing occurring at a lift coefficient of about 0.3. The same figure indicates that the cranked wing is ineffective insofar as eliminating the pitchup is concerned, although the lift coefficient at which the intability begins to occur is somewhat higher for the cranked wing. Subsequent plots of C_m against C_L for the cranked wing with extensions (figs. 6 to 9) indicate that the instability is eliminated by the addition of the trailing-edge inserts. For example, the 200_{50}, 133_{70}, and 200_{70} trailing-edge configurations all have good longitudinal stability characteristics. For the cases herein where wing trailing-edge modifications eliminated pitchup for the cranked wings, this pitchup was also eliminated for the uncranked cases with the identical modifications (from unpublished results). Thus, unless there were additional considerations, there would be little in favor of the cranked wing as compared with a low-aspect-ratio conventional wing.

Aerodynamic Efficiency

Minimum drag.- In figure 11 is presented the variation in minimum drag coefficient with trailing-edge extension for the various configurations tested. Examination of this figure indicates that increasing the amount of trailing-edge extension results in a decrease in $C_{D,min}$ and generally an increase in $\left(C_{D,b}\right)_{min}$ (indicative of the change in actual drag force). These changes in minimum drag with increasing amounts of trailing-edge extension reflect the combined effects of the changes in base pressure acting on the trailing edge and the higher skin-friction drag due to the larger surface area.

At M = 1.41, both the $0\text{-}200_{50}$ and $67_{50}\text{-}200_{50}$ configurations have approximately the same minimum drag as the basic cranked wing-body (0-0) and have only a slightly higher drag than the basic configuration at M = 2.01. Apparently, then, the decrease in wave drag for the 67_{50} leading-edge configuration (as compared to the 0 leading-edge configuration) is offset by the increased skin friction for the wing with the larger area.

Lift-curve slope.- The variation of lift-curve slope with trailing-edge extension is presented in figure 12. As can be seen in the basic data figures (figs. 6 to 9) the variation of lift coefficient with angle of attack is essentially linear up to α of about 6° to 8°, and it was over this linear portion of the curve that the values of C_{L_α} presented in figure 12 were obtained. It is seen from figure 12 that as the trailing-edge extension is increased, a reduction in lift-curve slope results when C_L is based on the respective wing areas (primarily due to the reduction in aspect ratio), but an increase in lift-curve slope results when the common area of the basic wing is used to nondimensionalize the lift. As might be expected, the configurations with the 200_{70} trailing edge produced the largest lift forces of all those tested.

Drag due to lift.- The drag-due-to-lift parameter, $\frac{C_D - C_{D,min}}{C_L{}^2}$, is presented in figure 13 as a function of trailing-edge extension. The values of $\frac{C_D - C_{D,min}}{C_L{}^2}$ were obtained from the slope of the curve of C_D slotted against $C_L{}^2$ which was essentially linear over the same range as the lift curve ($\alpha = 6^\circ$ to 8°) which in every case is beyond the C_L for $(L/D)_{max}$. Examination of figure 13 indicates that generally the drag-due-to-lift parameter is represented closely by the reciprocal of the lift-curve slope (with α in radians) indicating that the expected leading-edge suction is not realized and that the resultant-force vector due to incidence acts normal to the chord. When the coefficients are based on the individual wing areas, the drag-due-to-lift parameter increases with increasing amounts of trailing edge extension; however, when the coefficients are based on a common area, the result is that as larger trailing-edge extensions are added, the drag-due-to-lift parameter decreases (fig. 13(b)). Thus the configurations with trailing-edge extensions will produce a given lift force with less drag force due to lift than the basic cranked wing. This result arises from the increase in $C_{L_{\alpha,b}}$ with trailing-edge extension making it possible to maintain the same lift at a lower angle of attack with the extended trailing-edge configurations.

Maximum lift-drag ratio.- Values of maximum lift-drag ratio are presented in figure 14 where it is seen that for a particular leading-edge configuration, the net effect of increasing the trailing-edge extension is to increase $(L/D)_{max}$. For the case of no leading-edge suction, the maximum lift-drag ratio can be determined by the expression $(L/D)_{max} = 0.5\sqrt{\frac{C_{L_\alpha}}{C_{D,min}}}$ where C_{L_α} is per radian. Thus, with increasing trailing-edge extension, the reduction in C_{L_α} is more than offset by the reduction in $C_{D,min}$ resulting in increased $(L/D)_{max}$. It can also be noted in figure 14 that for the same trailing-edge extension, the 67_{50}-X configurations have about the same $(L/D)_{max}$ as the 0-X configurations. At both Mach numbers, the trailing-edge extensions were successful in increasing $(L/D)_{max}$ up to about 15 percent over that of the basic cranked wing.

Application of Results

In actual practice, the final selection of the best configuration would depend on the purpose for which the airplane was to be designed. For example, for a high-speed interceptor, the desirability of a low-drag configuration might outweigh that of having a high $(L/D)_{max}$, whereas for a long-range bomber it would be of primary importance to have a high $(L/D)_{max}$ with sufficient wing volume for carrying sufficient fuel for a long-range mission.

For the present case of wing-body combinations, the fact that the drag-due-to-trim is unknown introduces an uncertainty into the choice of the best configuration. However, for the purposes of the present discussion it will be assumed that the comparison will be made for operation at $(L/D)_{max}$ with neutral stability. Results of this comparison indicate that the 67_{50}-20_{50} configuration is attractive, particularly for C_D at $M = 1.41$, and C_L and $(L/D)_{max}$ at $M = 2.01$ as indicated in the following table.

Configuration	M	Percentage difference from basic configuration			
		Exposed-wing volume	C_D	C_L	$(L/D)_{max}$
67_{50}-200_{50}	1.41	85	-7	8	15
	2.01	85	2	21	19

L
2
6
1

As a matter of interest, the condition for operating at $(L/D)_{max}$ for the 67_{50}-200_{50} configuration corresponds to a wing loading of 100 lb/sq ft at 53,000 feet at M = 2.01 and at 40,000 feet at M = 1.41. Slightly higher gains in $(L/D)_{max}$ (at M = 2.01) and considerable gains in lift (at both Mach numbers) resulted with the 67_{50}-200_{70} configuration, but these gains were accompanied by increases in drag of 15 to 20 percent. As discussed previously, the final selection of the "best" configuration (even in the present simplified case) would depend on which aerodynamic characteristics were of primary interest.

One additional point remains to be emphasized; namely, that the data presented herein were obtained with relatively crude models designed to facilitate the testing of a large number of configurations with a minimum of construction effort. The results are therefore to be applied more for indicating trends than for the specific numbers presented since, with the use of more refined airfoil sections, wing twist and camber, and improved body design, it is believed that significant increases in maximum lift-drag ratio and reductions in drag could be realized.

CONCLUDING REMARKS

An investigation has been conducted in the Langley 4- by 4-foot supersonic pressure tunnel at Mach numbers of 1.41 and 2.01 to determine the effects of certain plan-form variations on the aerodynamic characteristics of a family of cranked wings in combination with an ogive-cylinder body of revolution.

Results of the tests indicate that the best overall characteristics were obtained with the low-aspect-ratio wings. Plan-form changes which involved decreasing the aspect ratio resulted in higher values of maximum lift-drag ratio in addition to large increases in wing volume. Indications are that this trend would have continued to exist at aspect ratios even lower than the lowest considered in the present tests. Increases in the maximum lift-drag ratio of about 15 percent over the basic wing were achieved with practically no increase in drag.

The severe longitudinal instability associated with the basic cranked wing was no longer present (within the limits of the present tests) on the lower-aspect-ratio wings formed by sweeping forward the inboard portion of the trailing edge.

Langley Research Center,
National Aeronautics and Space Administration,
Langley Field, Va., August 18, 1959.

REFERENCES

1. Fischetti, Thomas L.: Effects of Fences, Leading-Edge Chord-Extensions, Boundary-Layer Ramps, and Trailing-Edge Flaps on the Longitudinal Stability of a Twisted and Cambered 60° Sweptback-Wing-Indented-Body Configuration at Transonic Speeds. NACA RM L54D09a, 1954.

2. Cooper, Morton, and Sevier, John R., Jr.: Effects of a Series of Inboard Plan-Form Modifications on the Longitudinal Characteristics of Two 47° Sweptback Wings of Aspect Ratio 3.5, Taper Ratio 0.2, and Different Thickness Distributions at Mach Numbers of 1.61 and 2.01. NACA RM L53E07a, 1953.

3. Sevier, John R., Jr.: Investigation of the Effects of Body Indentation and of Wing-Plan-Form Modification on the Longitudinal Characteristics of a 60° Swept-Wing—Body Combination at Mach Numbers of 1.41, 1.61, and 2.01. NACA RM L55E17, 1955.

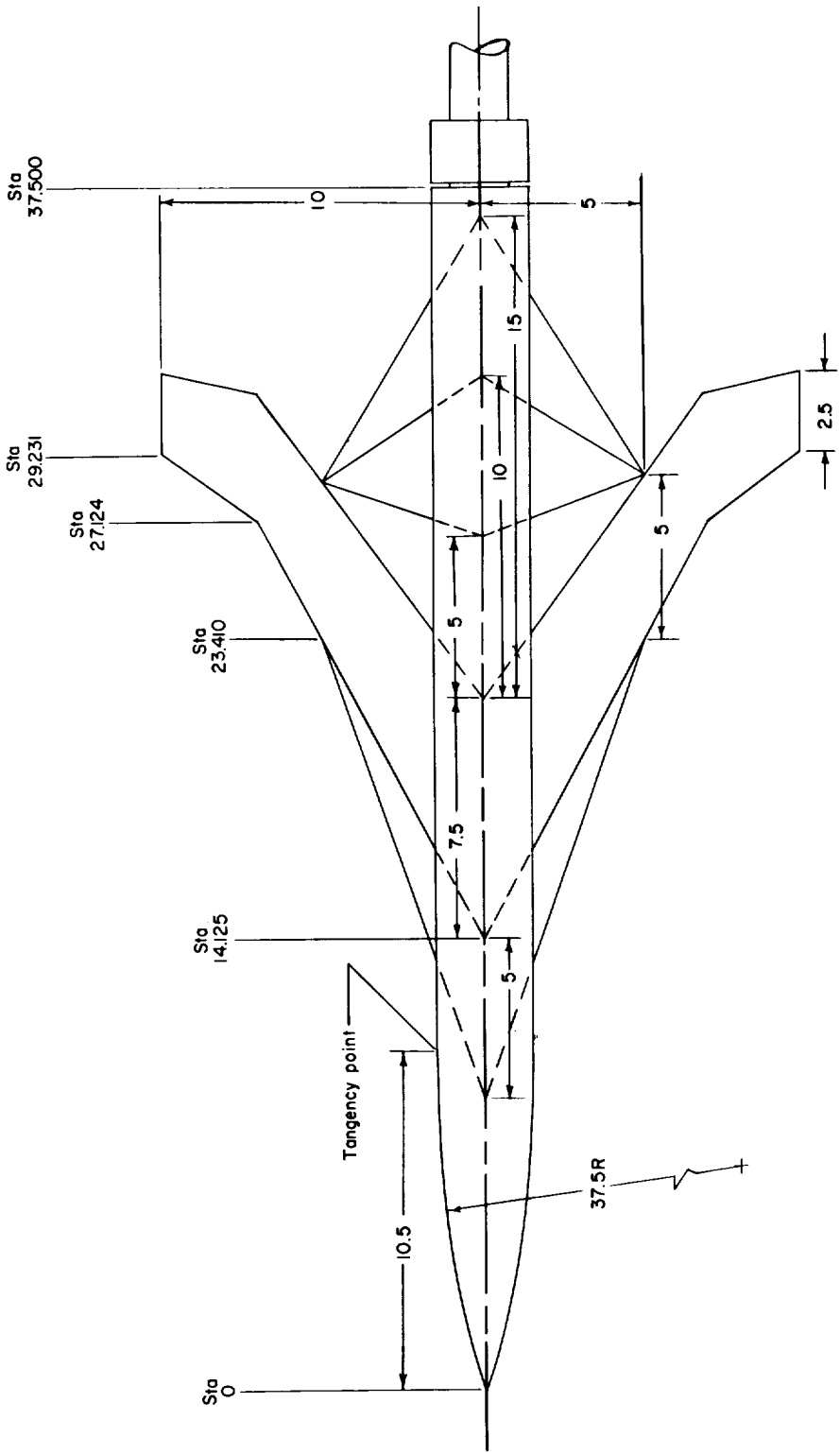

(a) Modifications extending to the 50-percent semispan.

Figure 1.- Schematic layout of model. (All dimensions are in inches unless otherwise noted.)

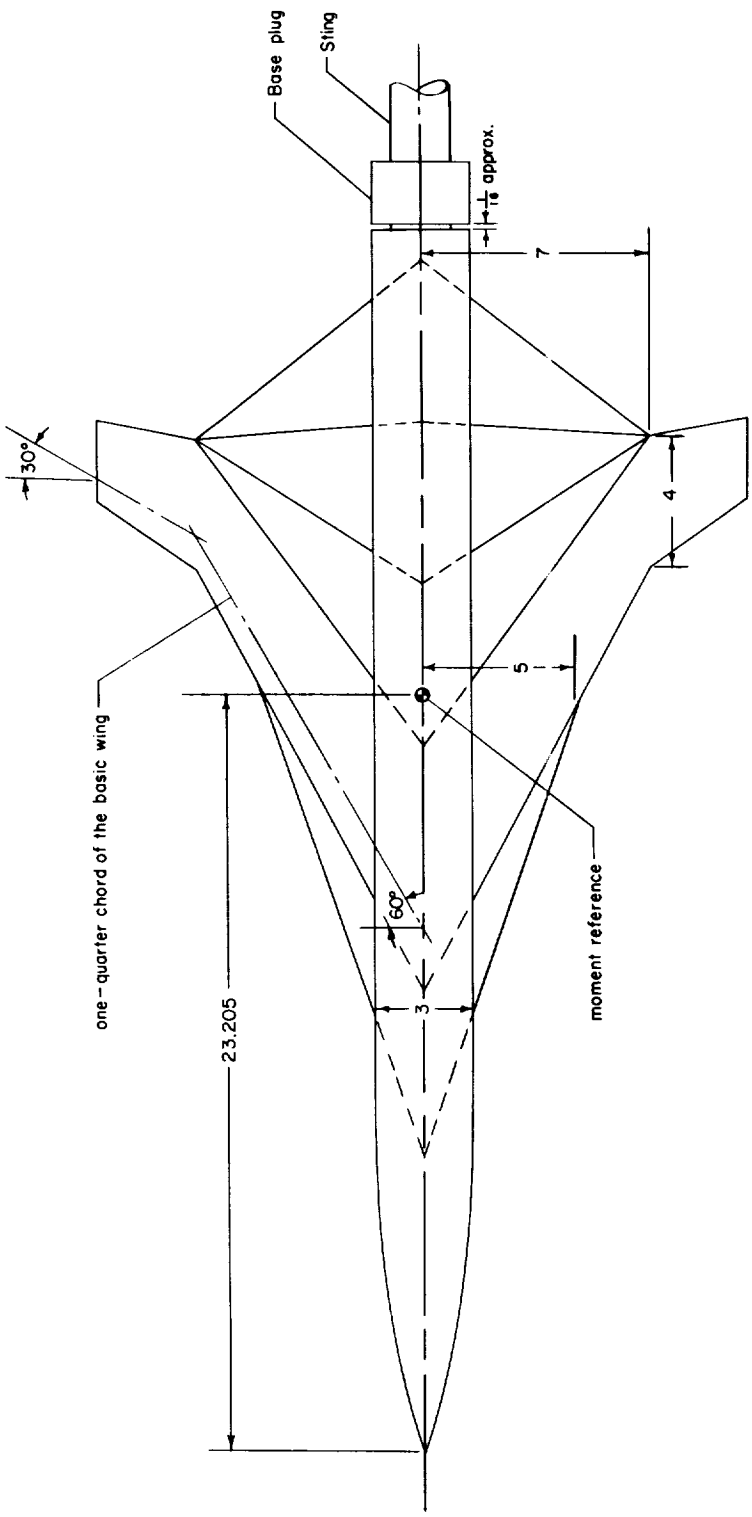

(b) Modifications extending to the 70-percent semispan.

Figure 1.- Concluded.

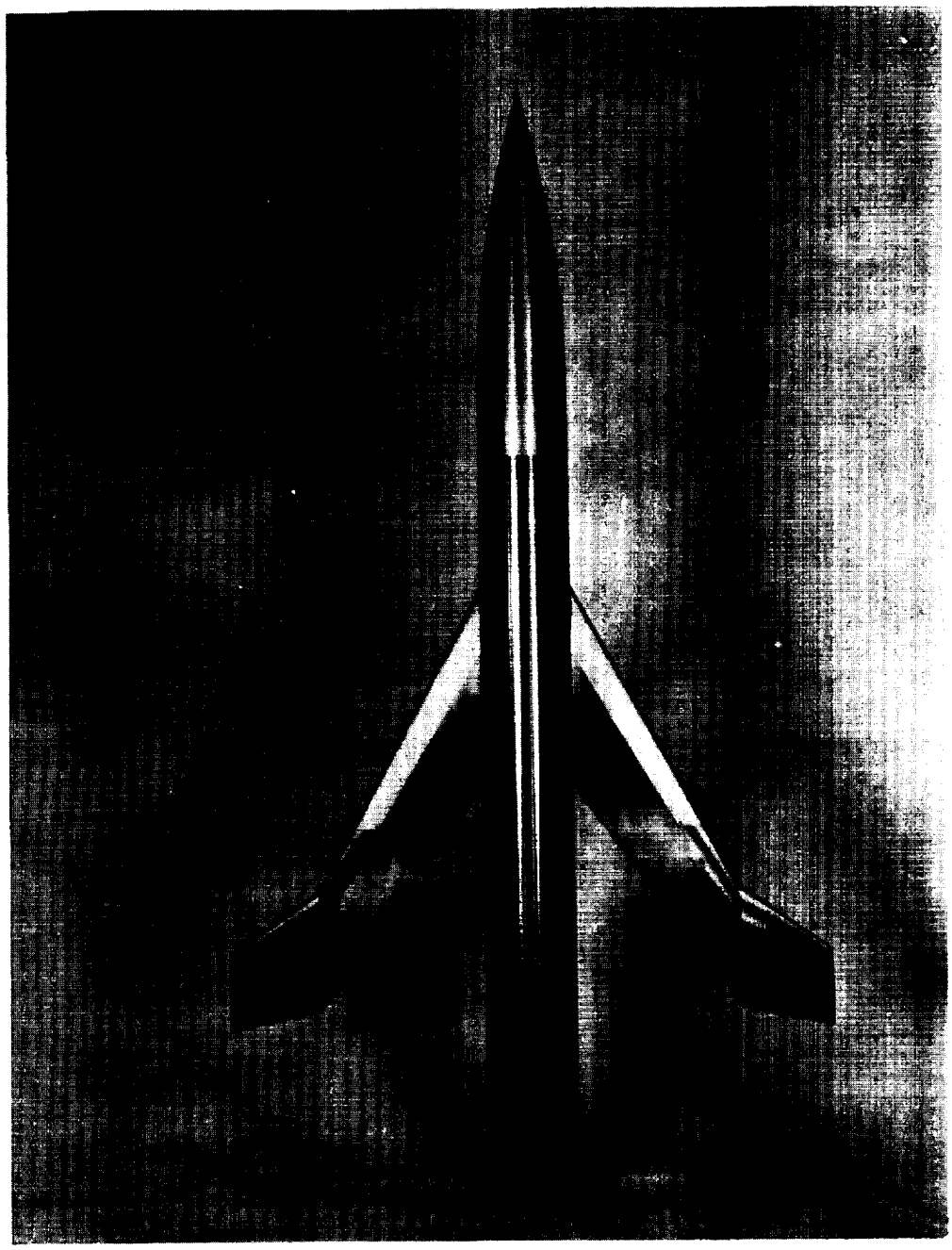

(a) Basic cranked wing (0-0) in combination with body. L-92318

Figure 2.- View of representative models.

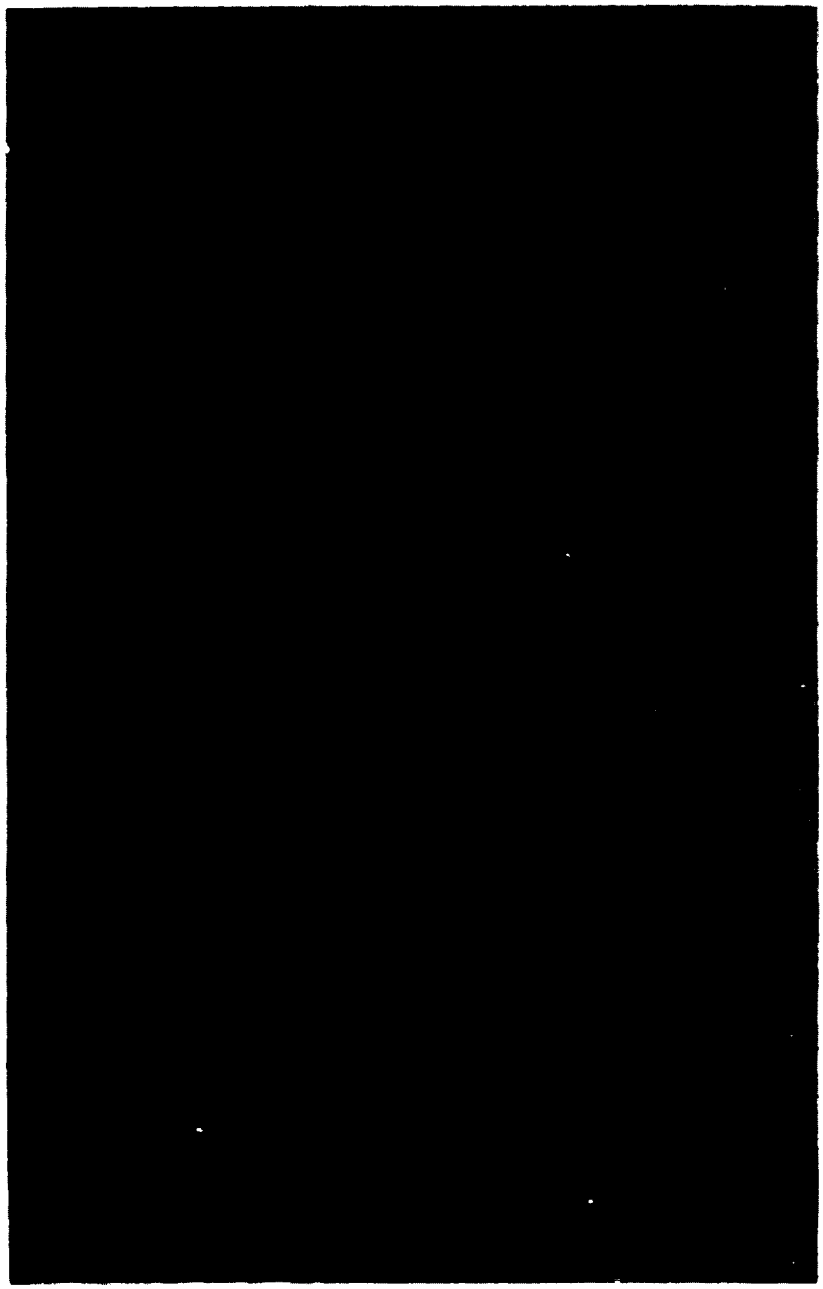

(b) The 67_{50}-200_{70} wing in combination with body. L-92320

Figure 2.- Concluded.

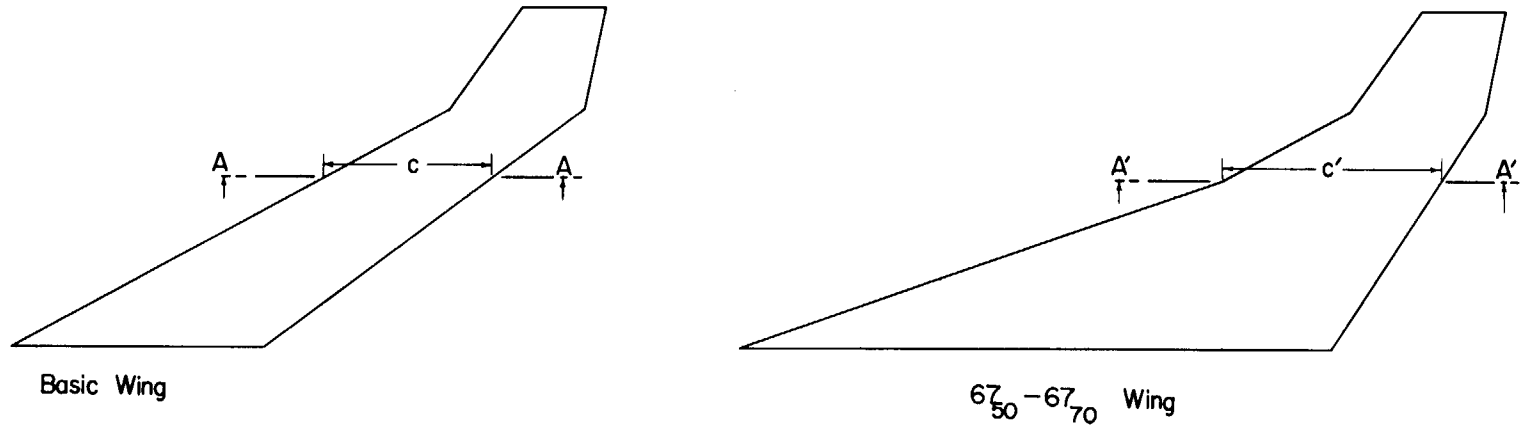

Figure 3.- Details of airfoil section.

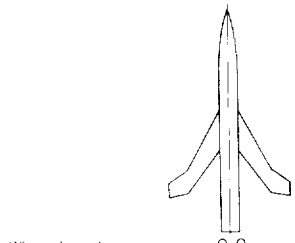

Wing designation	0-0
Area, sq ft	694
Mean aerodynamic chord, ft	452
Aspect ratio	4 000
Exposed wing volume, cu ft	0124

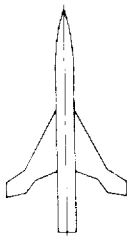

Wing designation	$0\text{-}67_{50}$
Area, sq ft	868
Mean aerodynamic chord, ft	639
Aspect ratio	3.204
Exposed wing volume, cu ft	0150

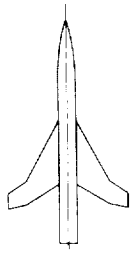

	$0\text{-}67_{70}$
	.938
	.680
	2.965
	.0168

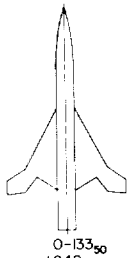

Wing designation	$0\text{-}133_{50}$
Area, sq ft	1.042
Mean aerodynamic chord, ft	.857
Aspect ratio	2.669
Exposed wing volume, cu ft	.0177

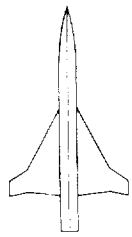

	$0\text{-}133_{70}$
	1.181
	.929
	2.352
	.0212

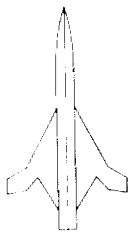

Wing designation	$0\text{-}200_{50}$
Area, sq ft	1.215
Mean aerodynamic chord, ft	1.091
Aspect ratio	2.289
Exposed wing volume, cu ft	.0203

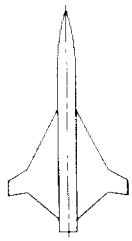

	$0\text{-}200_{70}$
	1.424
	1.187
	1.953
	.0256

(a) Basic (0) leading edge.

Figure 4.- Geometric details of models.

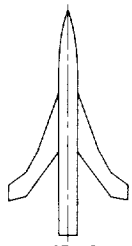

Wing designation	67_{50}–0
Area, sq ft	.868
Mean aerodynamic chord, ft	.639
Aspect ratio	3.204
Exposed wing volume, cu ft	.0150

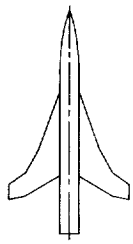

Wing designation	67_{50}–67_{70}
Area, sq ft	1.111
Mean aerodynamic chord, ft	.890
Aspect ratio	2.501
Exposed wing volume, cu ft	.0194

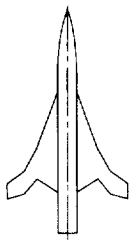

Wing designation	67_{50}–133_{50}
Area, sq ft	1.215
Mean aerodynamic chord, ft	1.091
Aspect ratio	2.289
Exposed wing volume, cu ft	.0203

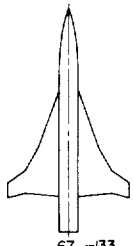

Wing designation	67_{50}–133_{70}
Area, sq ft	1.354
Mean aerodynamic chord, ft	1.151
Aspect ratio	2.055
Exposed wing volume, cu ft	.0238

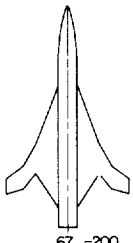

Wing designation	67_{50}–200_{50}
Area, sq ft	1.389
Mean aerodynamic chord, ft	1.336
Aspect ratio	2.000
Exposed wing volume, cu ft	.0229

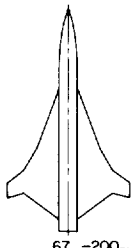

Wing designation	67_{50}–200_{70}
Area, sq ft	1.597
Mean aerodynamic chord, ft	1.416
Aspect ratio	1.740
Exposed wing volume, cu ft	.0282

(b) 67_{50} leading edge.

Figure 4.- Concluded.

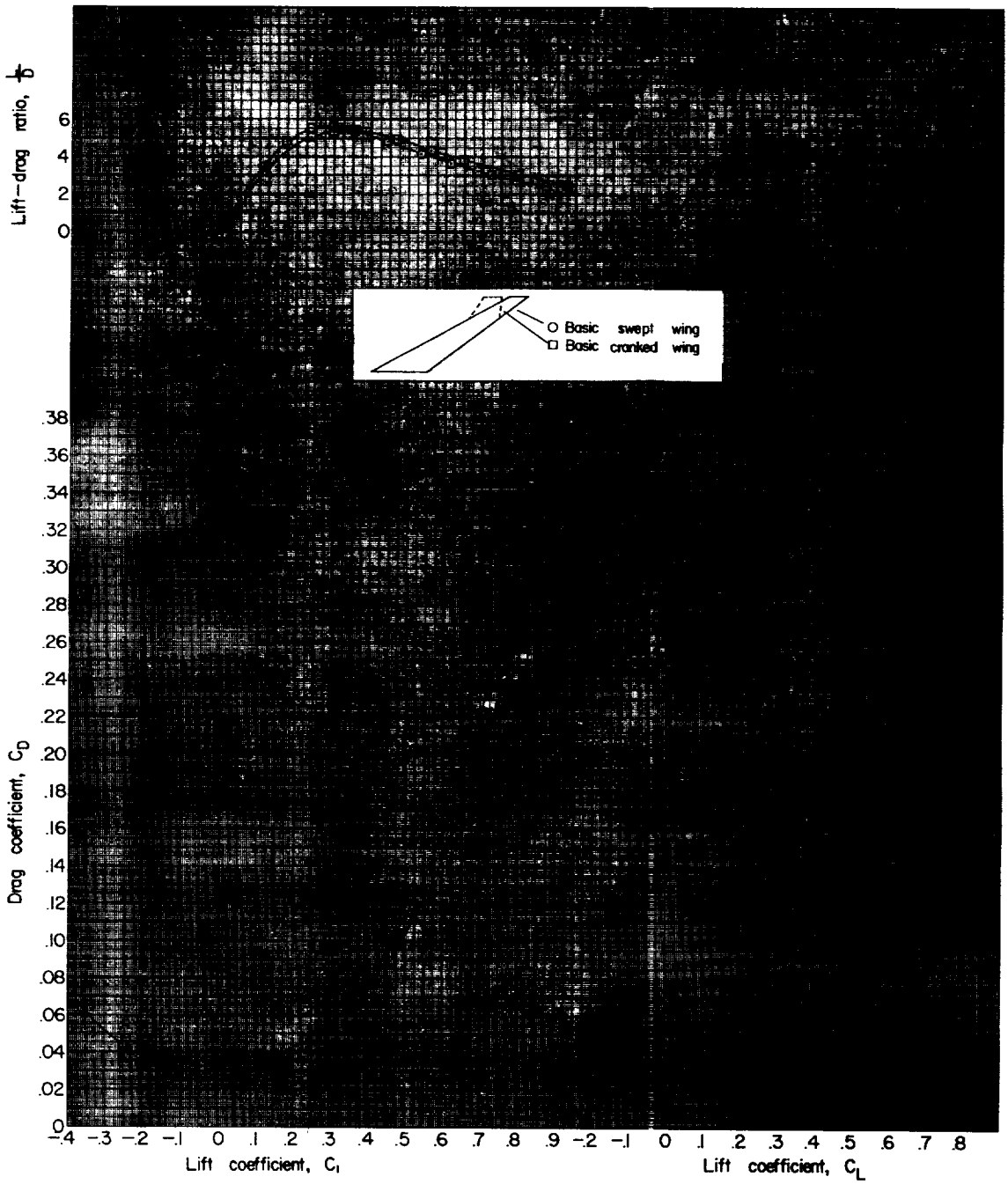

Figure 5.- Comparison of the aerodynamic characteristics of the swept and cranked wing-body combinations.

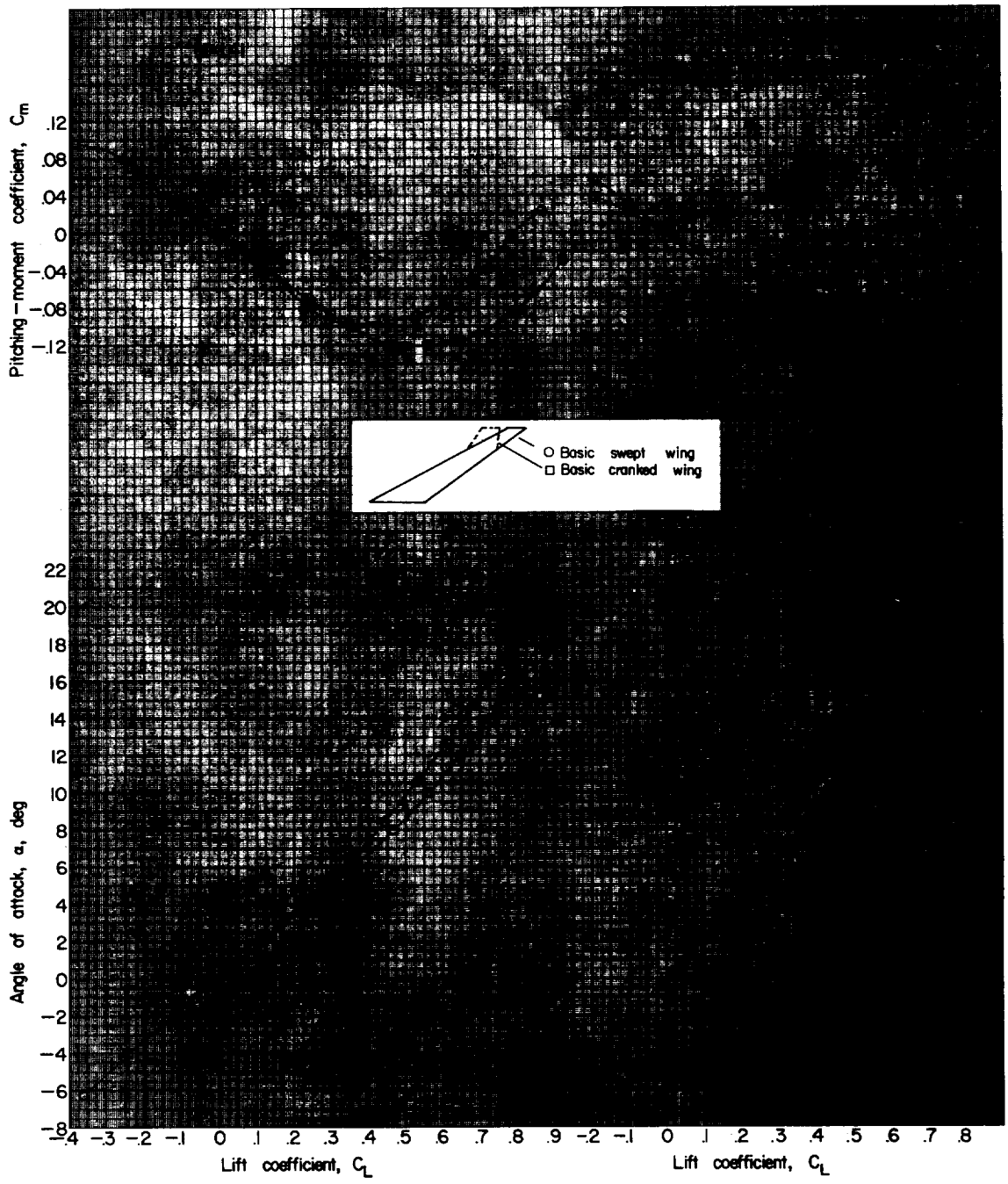

Figure 5.- Concluded.

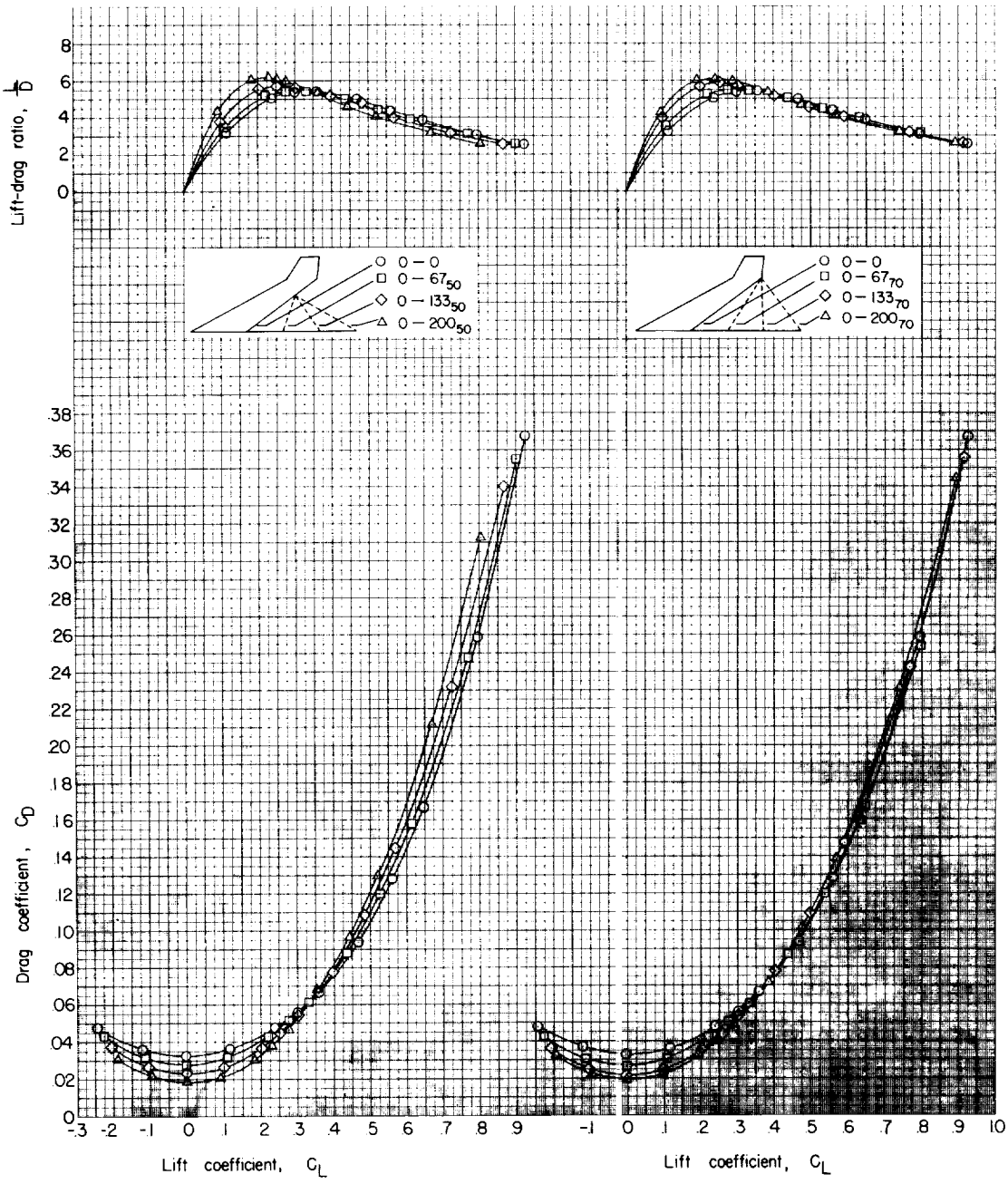

Figure 6.- Aerodynamic characteristics at M = 1.41 of the family of cranked wings (in combination with the body with the basic (0) leading edge).

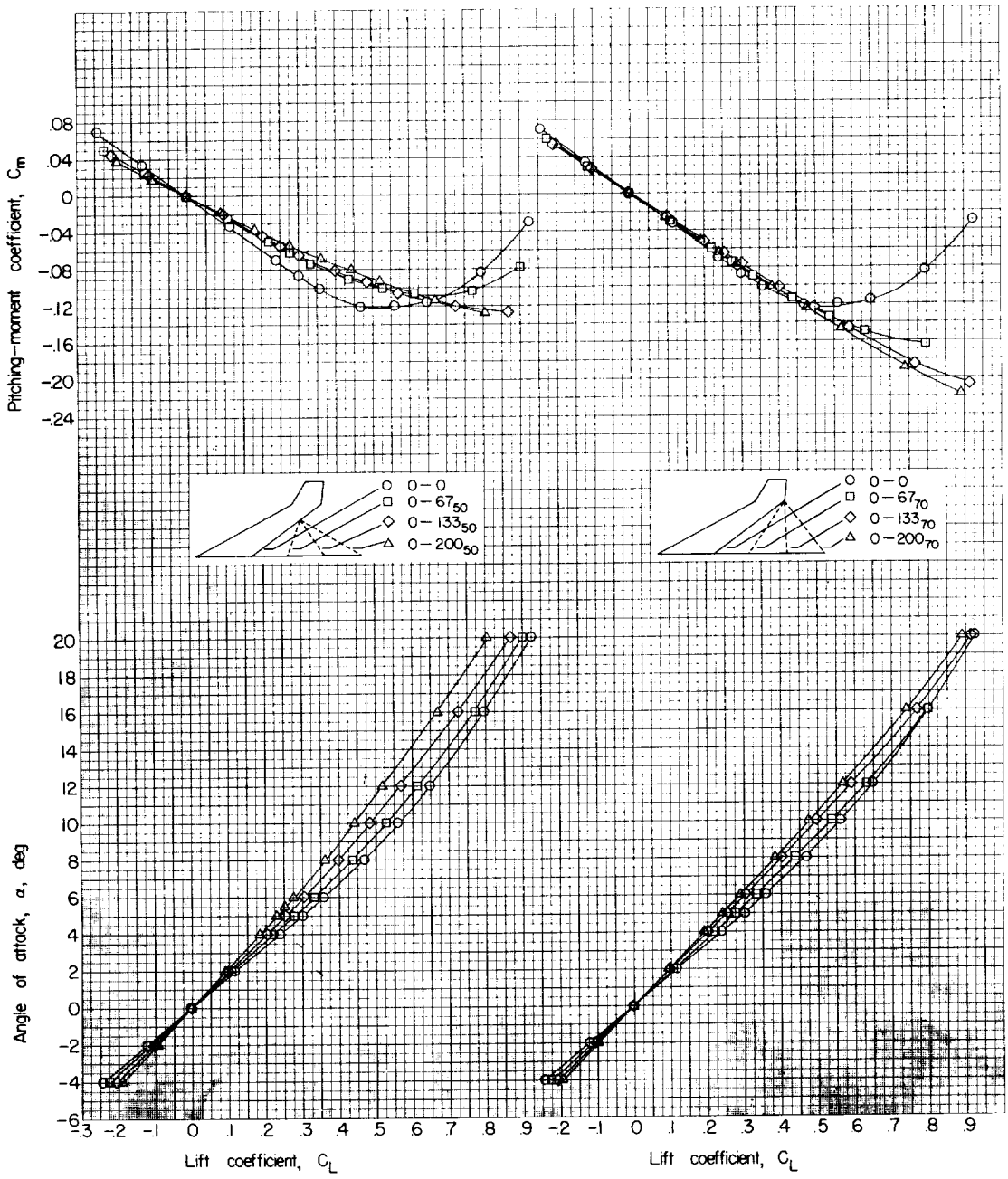

Figure 6.- Concluded.

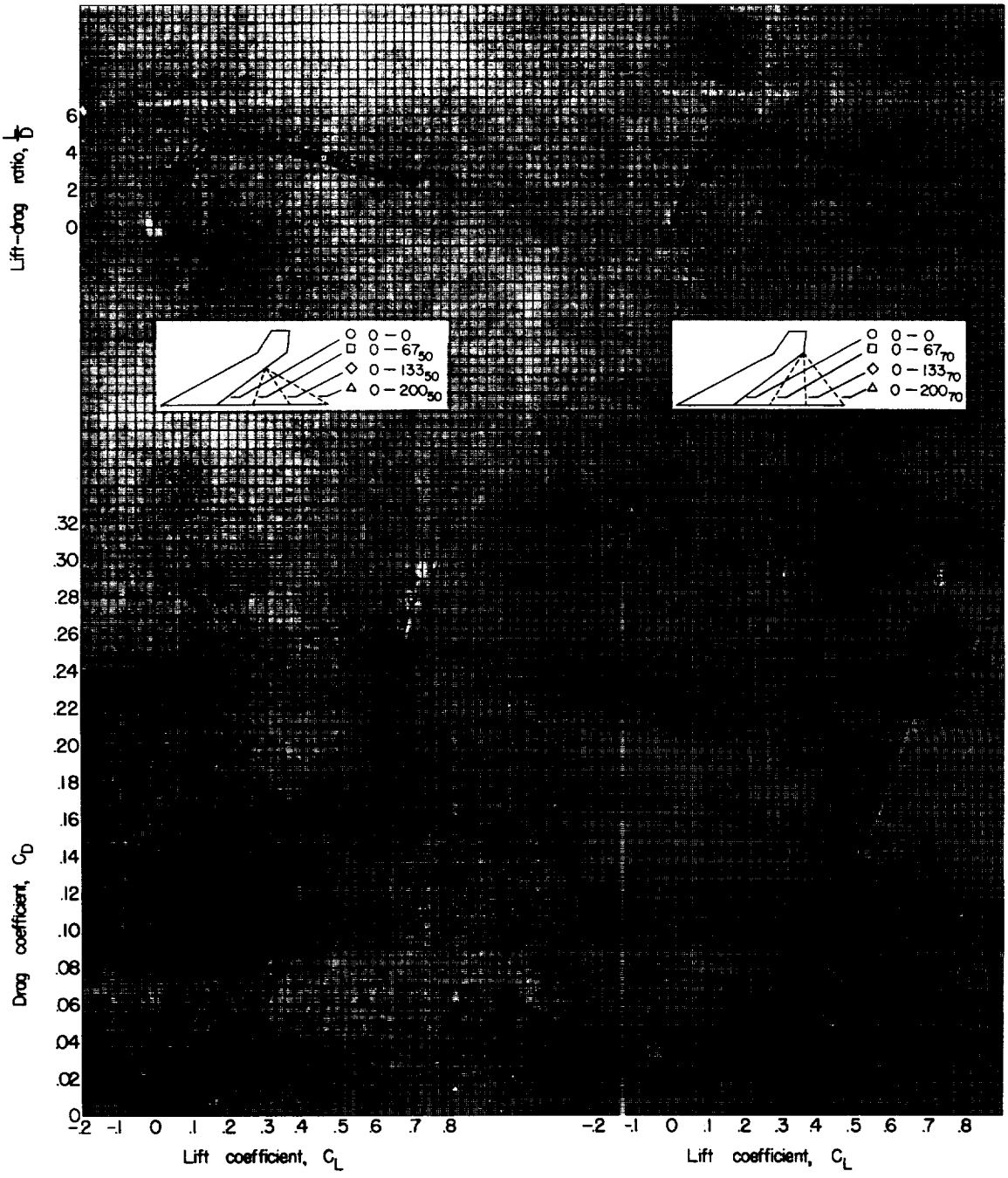

Figure 7.- Aerodynamic characteristics at M = 2.01 of the family of cranked wings (in combination with the body with the basic (0) leading edge).

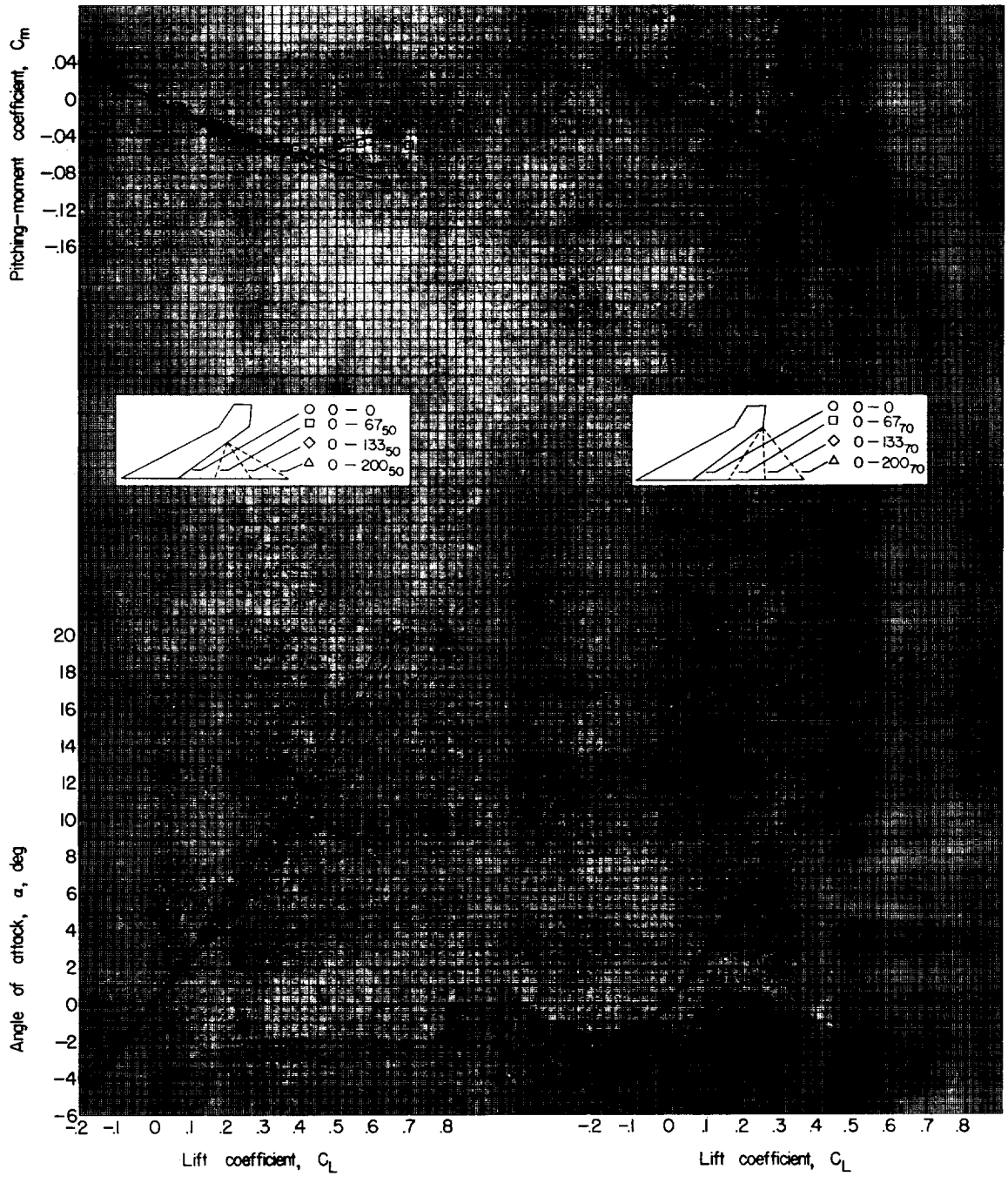

Figure 7.- Concluded.

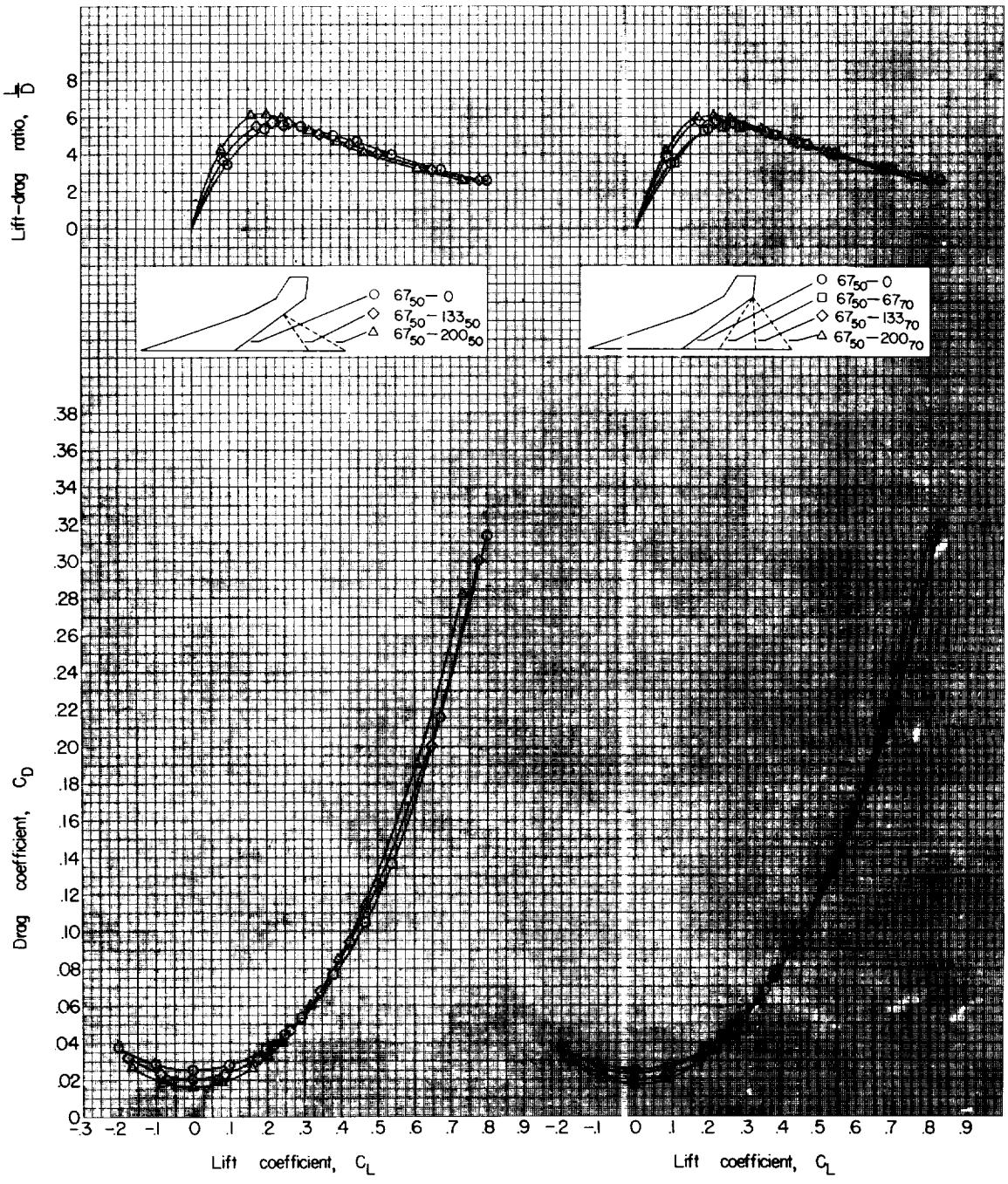

Figure 8.- Aerodynamic characteristics at M = 1.41 of the family of cranked wings (in combination with the body) with the 67_{50} leading edge.

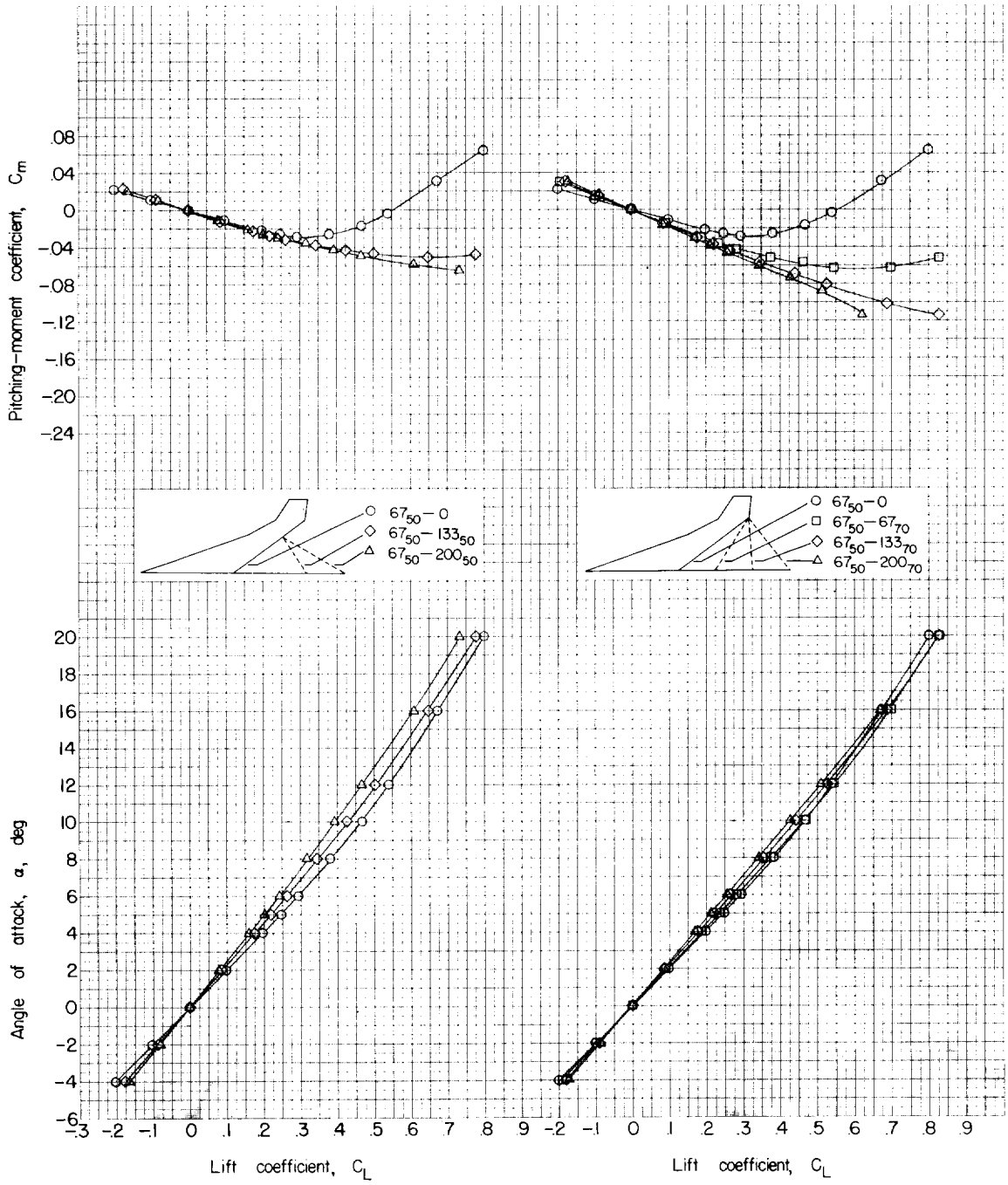

Figure 8.- Concluded.

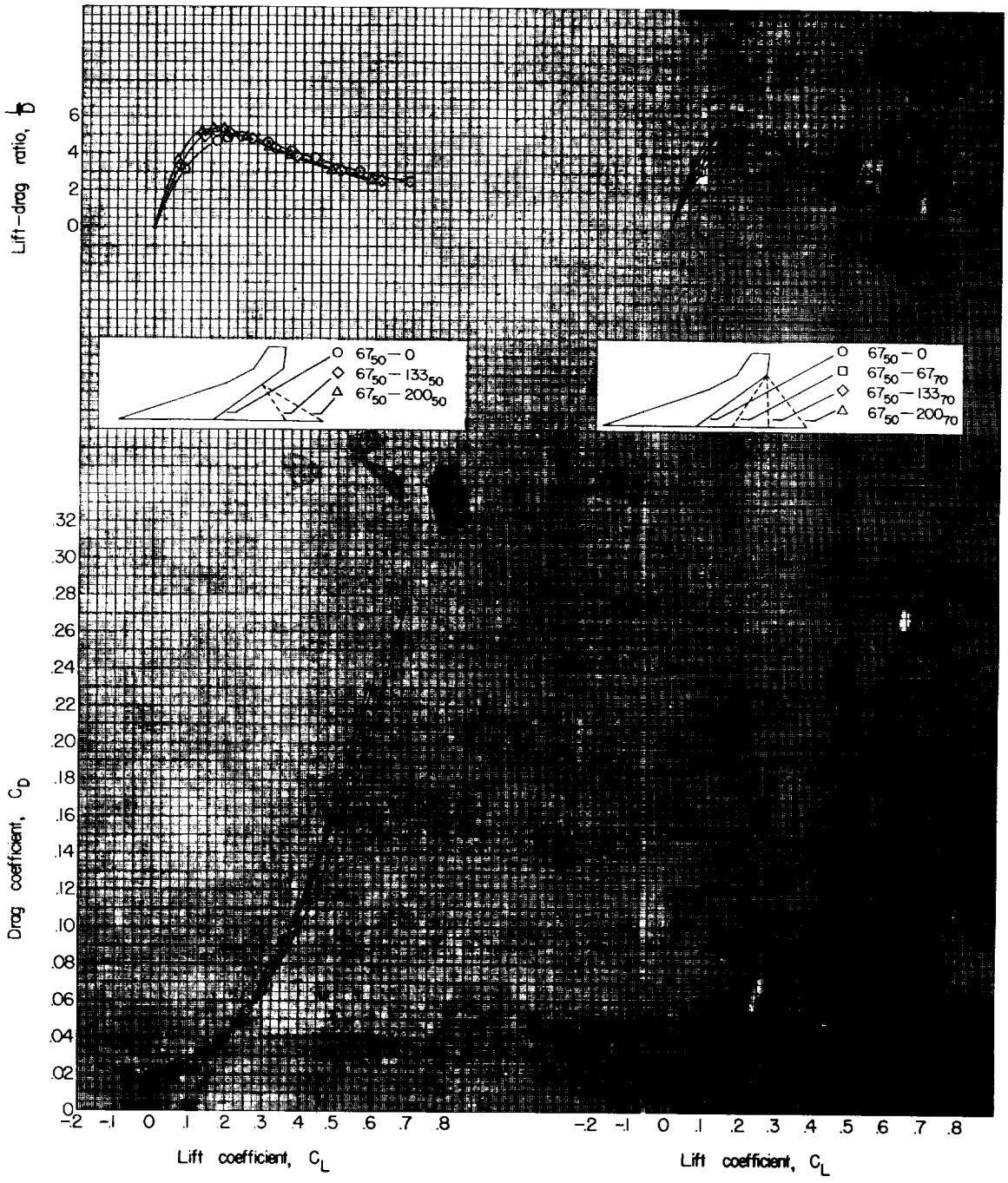

Figure 9.- Aerodynamic characteristics at M = 2.01 of the family of cranked wings (in combination with the body) with the 67_{50} leading edge.

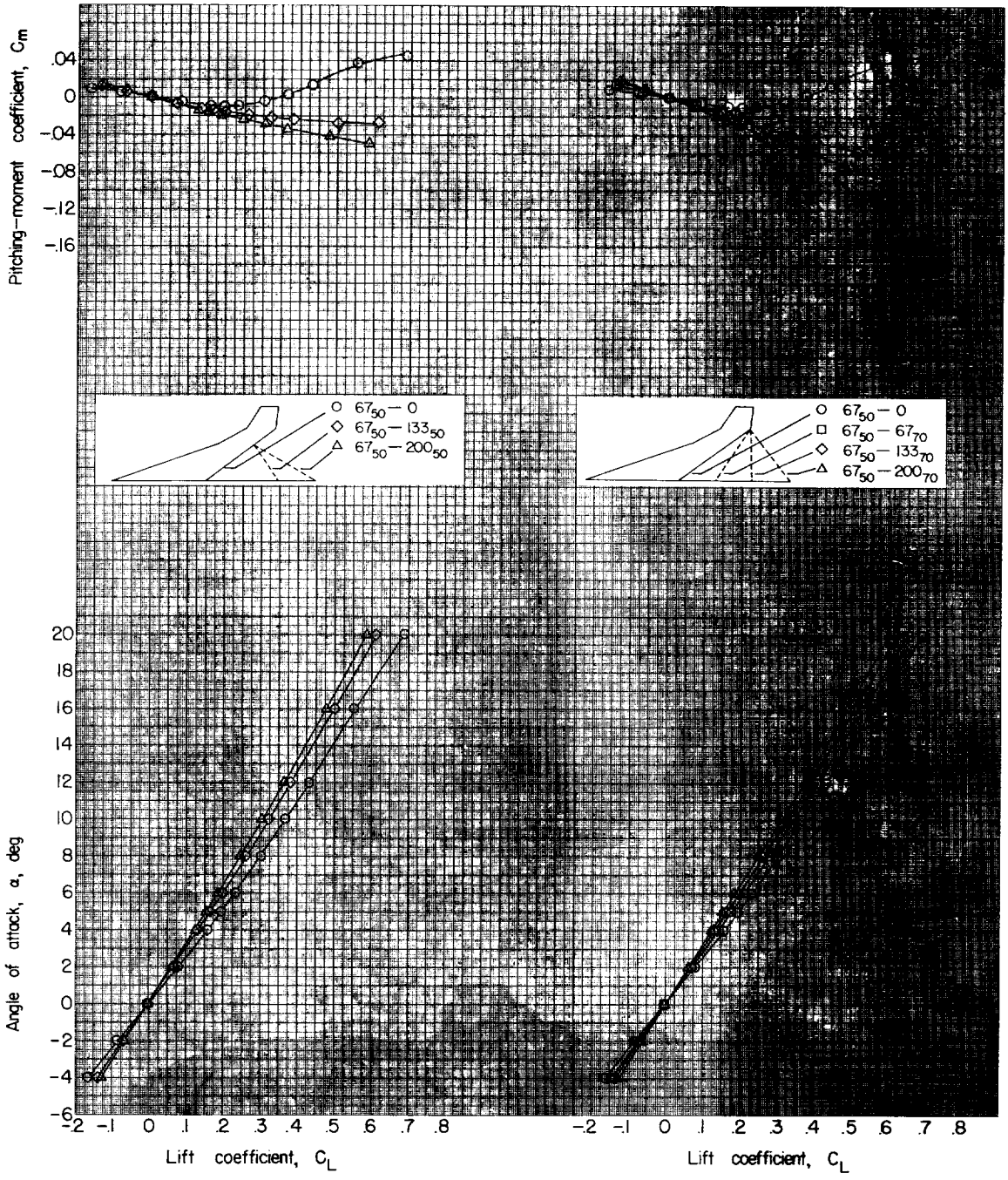

Figure 9.- Concluded.

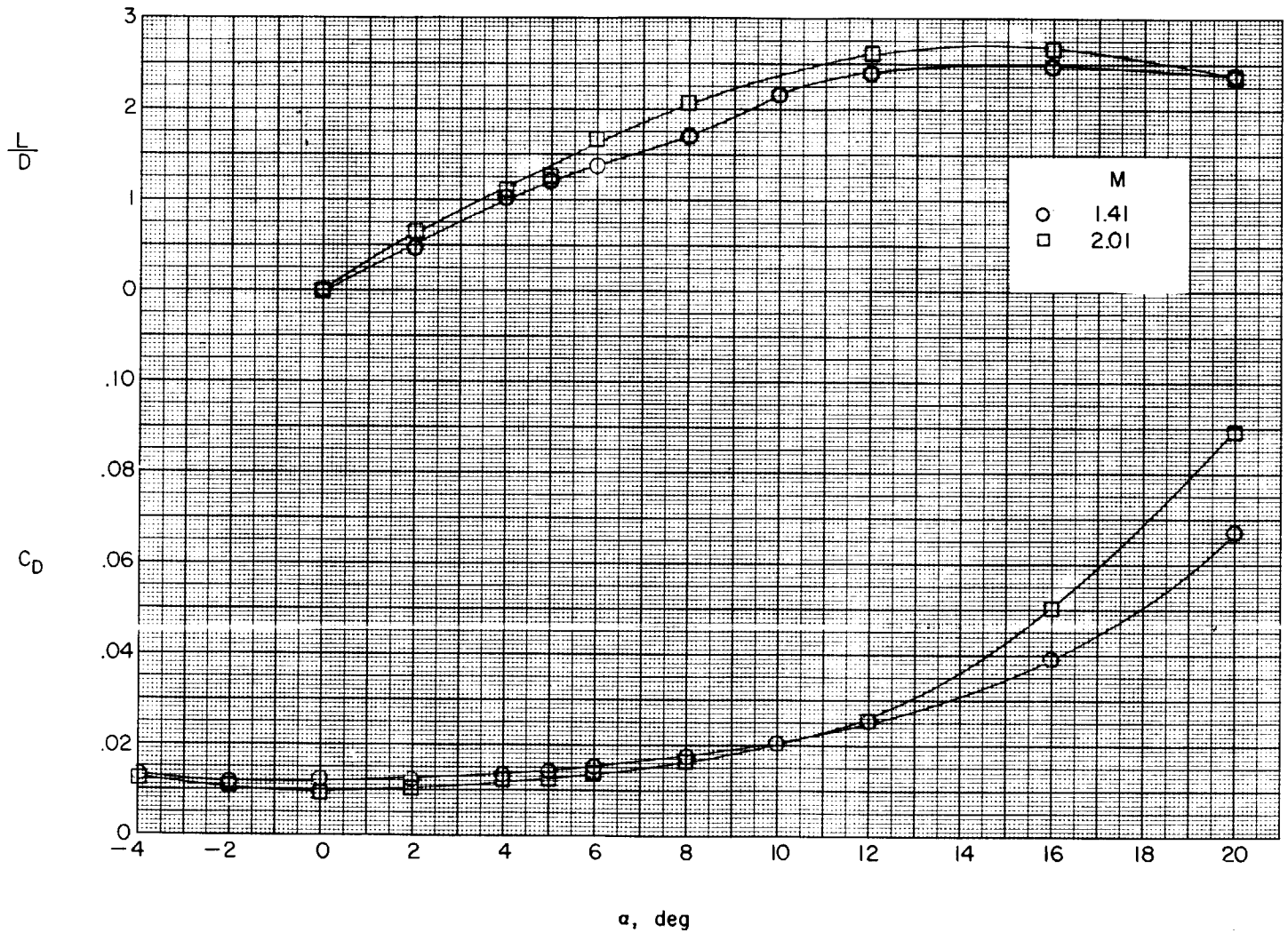

Figure 10.- Aerodynamic characteristics of the body alone. Coefficients are based on the geometry of the basic cranked wing and C_m is taken about $\bar{c}/4$ of the basic cranked wing.

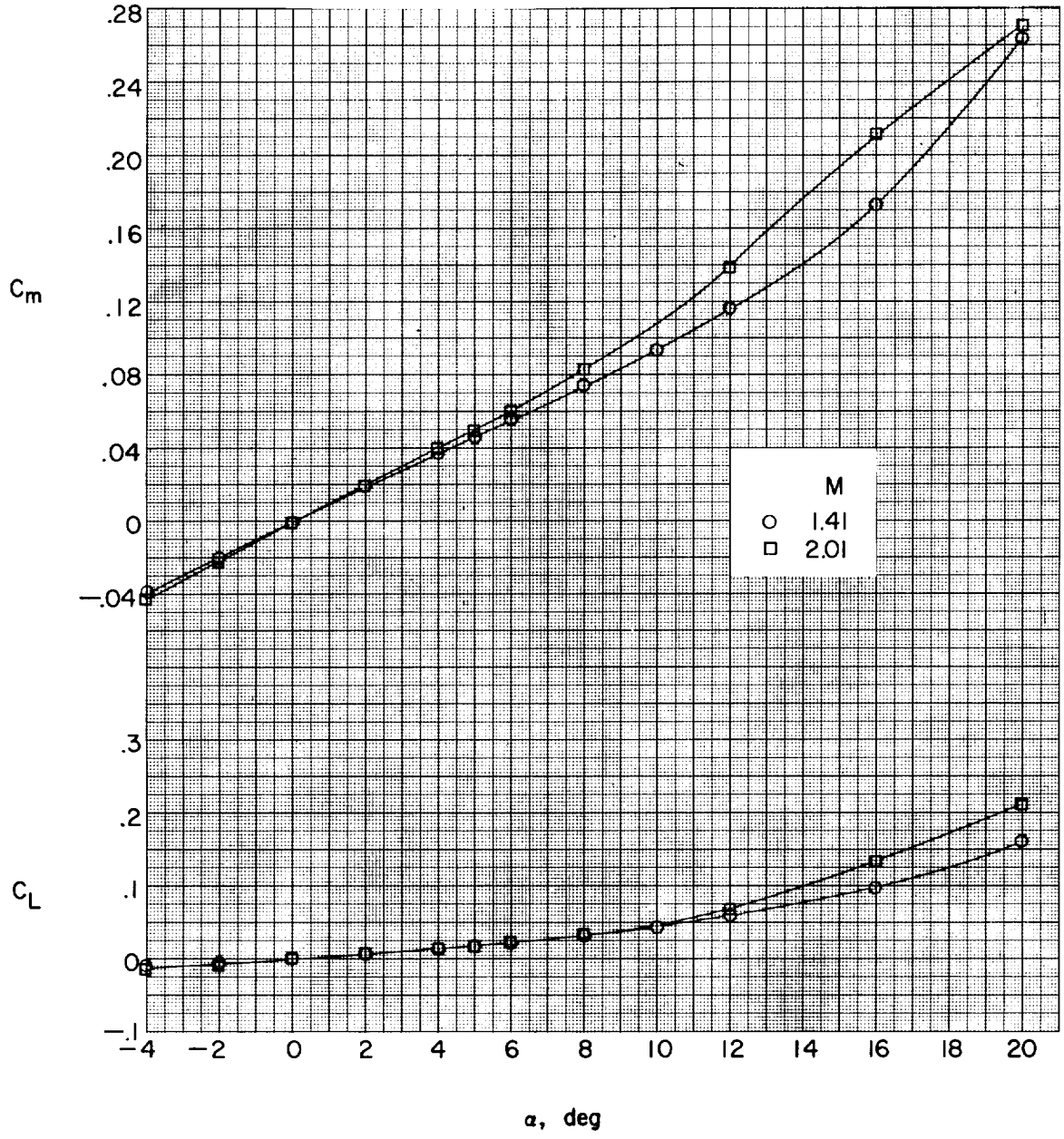

Figure 10.- Concluded.

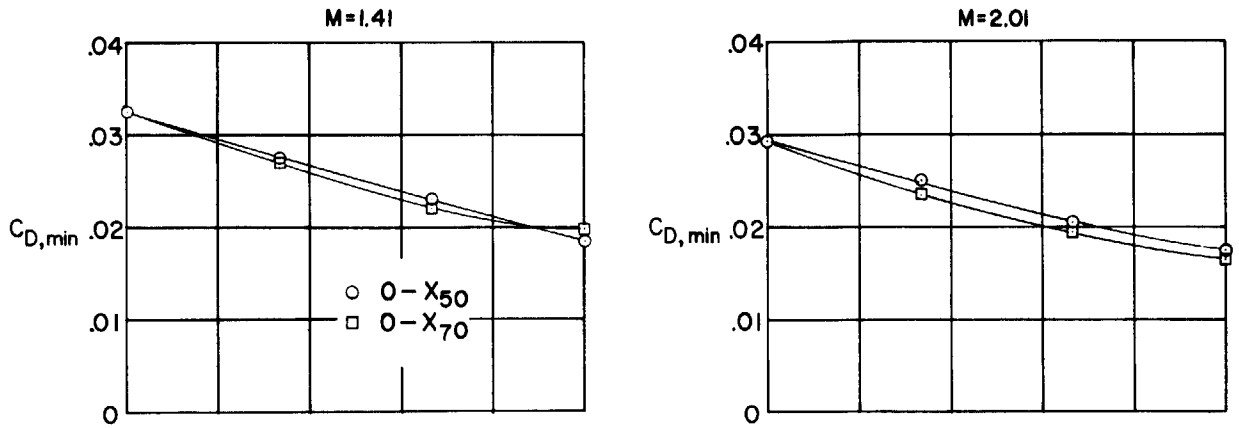

(a) Coefficients based on respective wing areas. Configurations 0-X_{50} and 0-X_{70}.

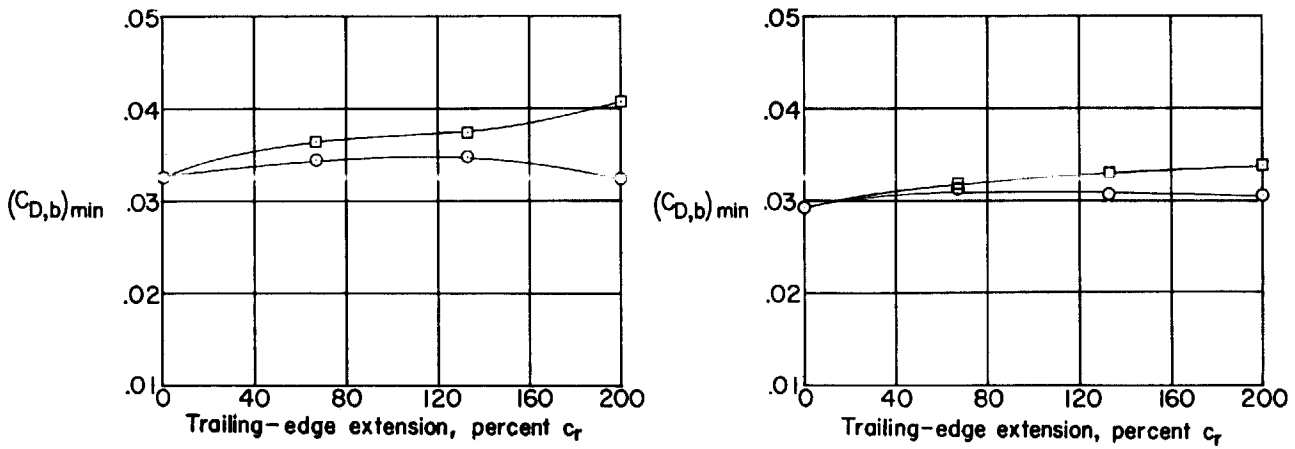

(b) Coefficients based on the area of the basic cranked wing. Configurations 0-X_{50} and 0-X_{70}.

Figure 11.- Minimum drag characteristics of the configurations tested.

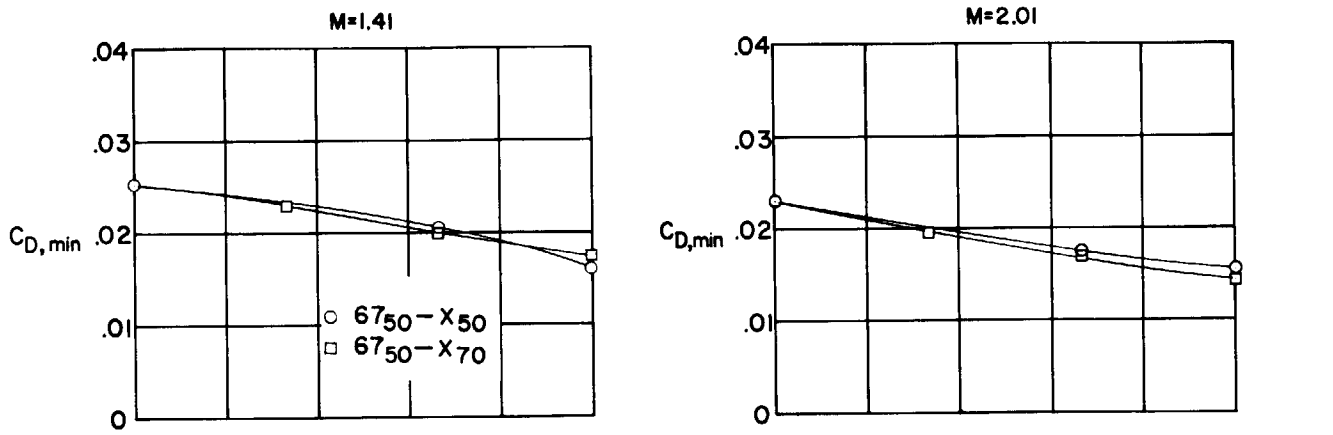

(c) Coefficients based on respective wing areas. Configurations 67_{50}-X_{50} and 67_{50}-X_{70}.

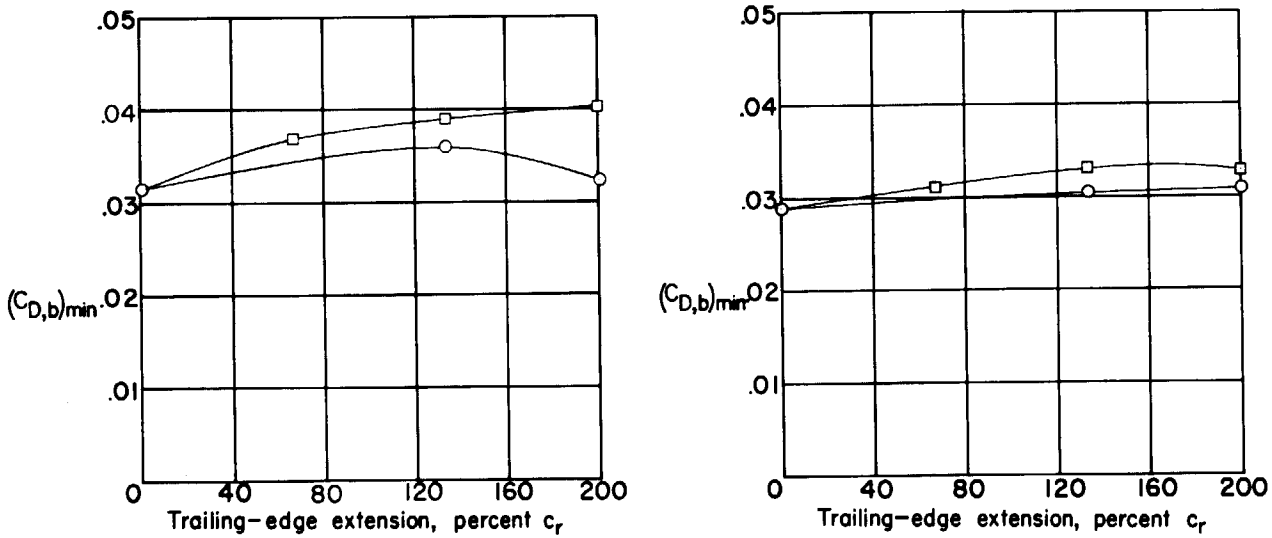

(d) Coefficients based on the area of the basic cranked wing. Configurations 67_{50}-X_{50} and 67_{50}-X_{70}.

Figure 11.- Concluded.

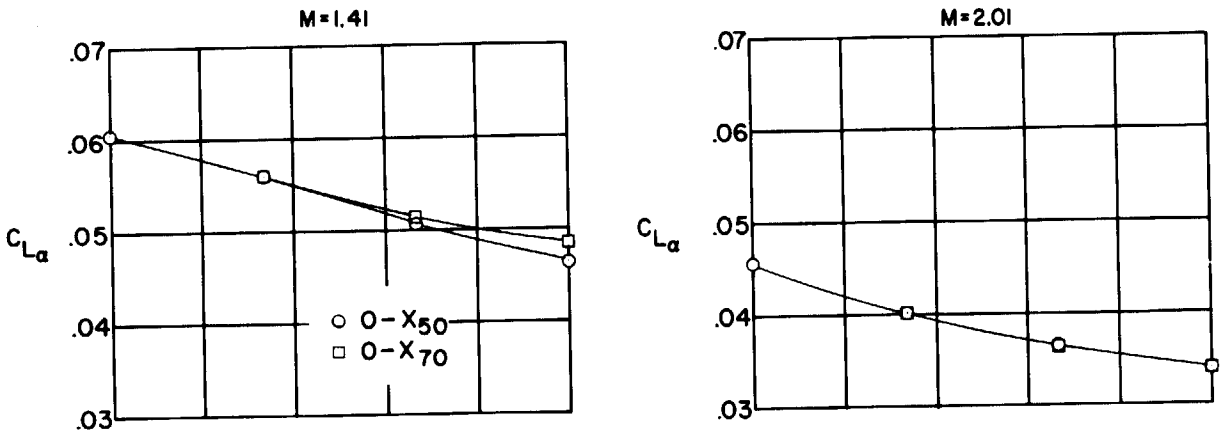

(a) Coefficients based on respective wing areas. Configurations 0-X_{50} and 0-X_{70}.

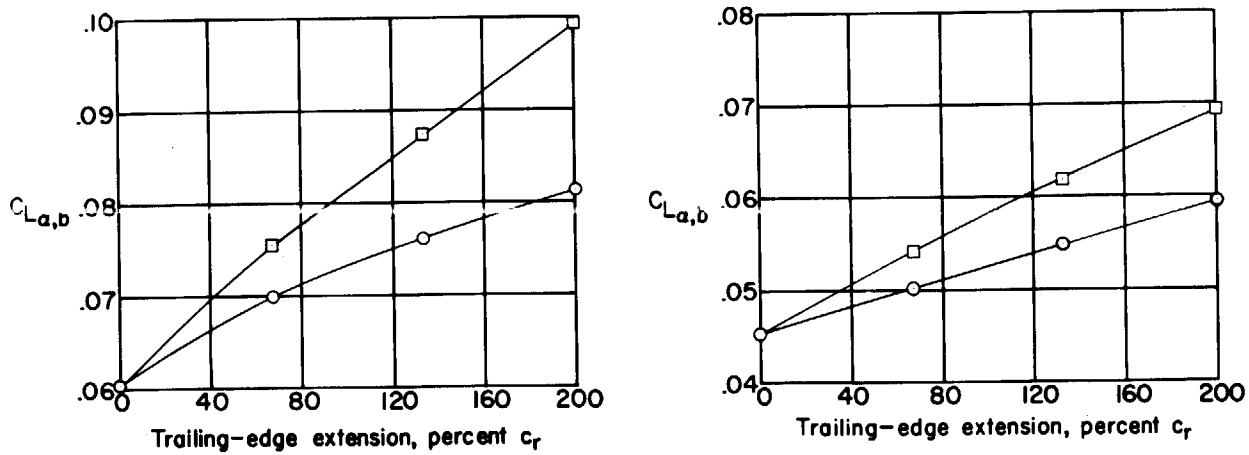

(b) Coefficients based on the area of the basic cranked wing. Configurations 0-X_{50} and 0-X_{70}.

Figure 12.- Lift-curve slopes of the configurations tested.

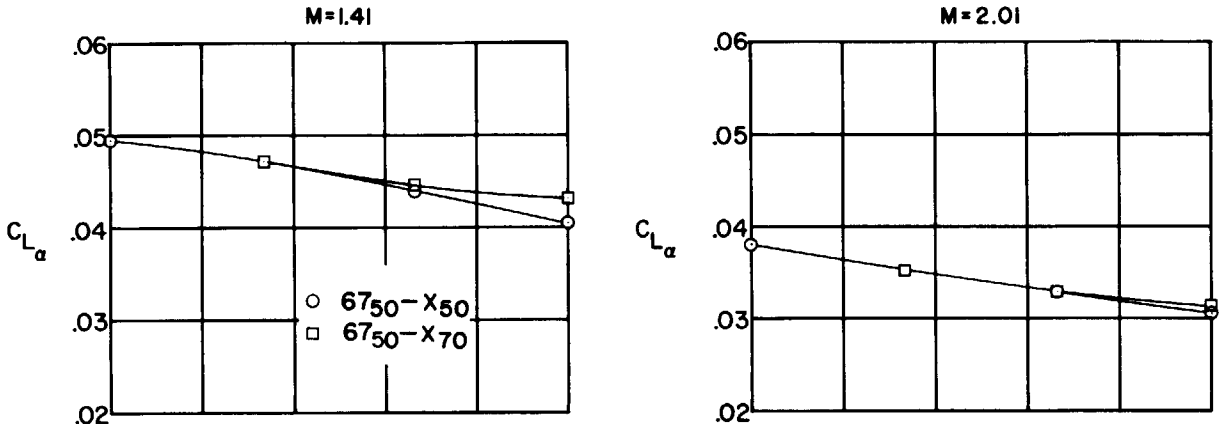

(c) Coefficients based on respective wing areas. Configurations 67_{50}-X_{50} and 67_{50}-X_{70}.

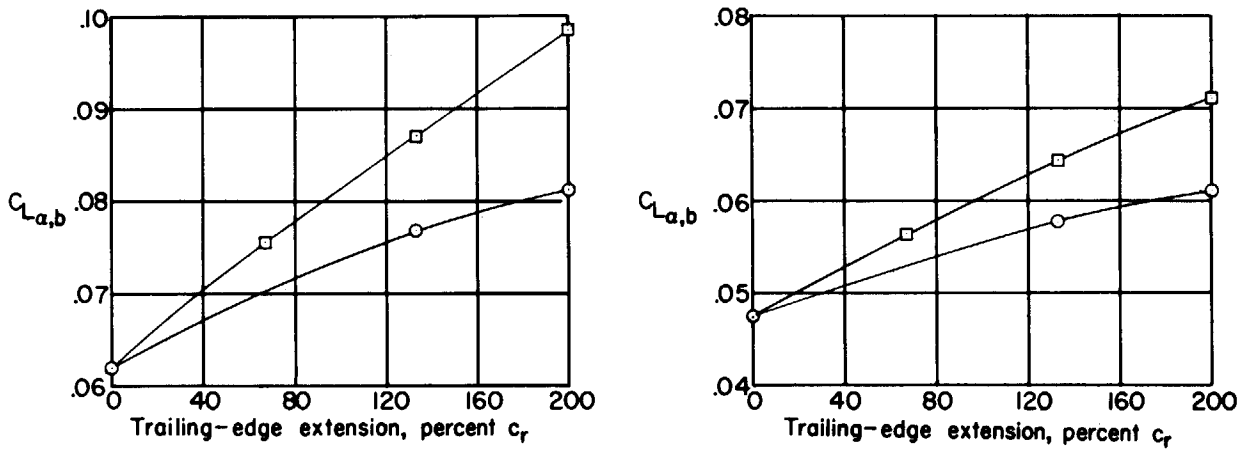

(d) Coefficients based on the area of the basic cranked wing. Configurations 67_{50}-X_{50} and 67_{50}-X_{70}.

Figure 12.- Concluded.

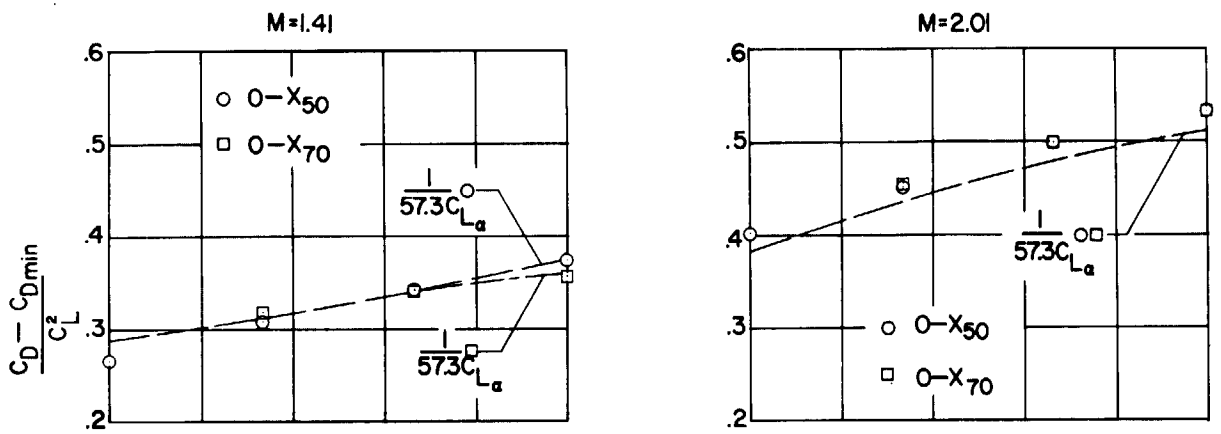

(a) Coefficients based on respective wing areas. Configurations 0-X_{50} and 0-X_{70}.

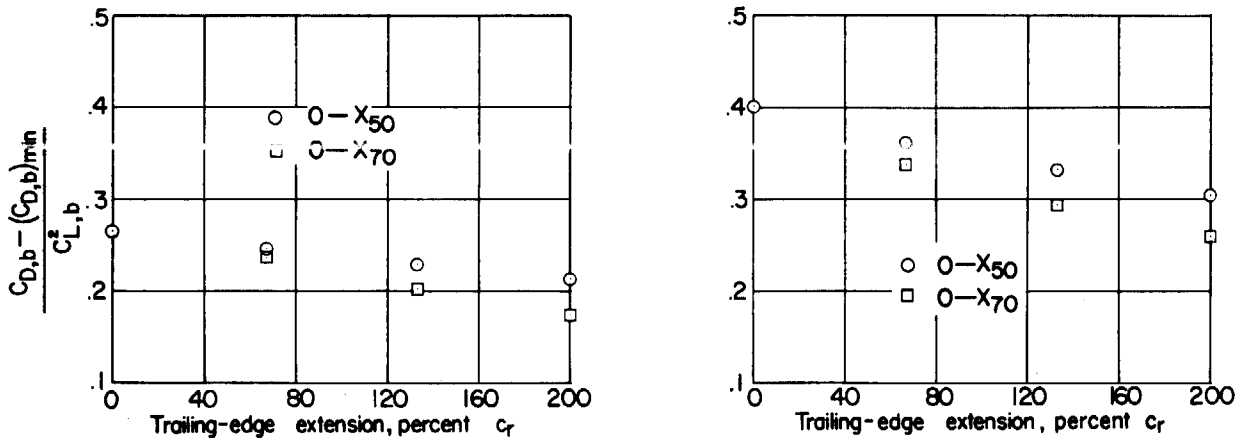

(b) Coefficients based on the area of the basic cranked wing. Configurations 0-X_{50} and 0-X_{70}.

Figure 13.- Drag-due-to-lift parameter of the configurations tested.

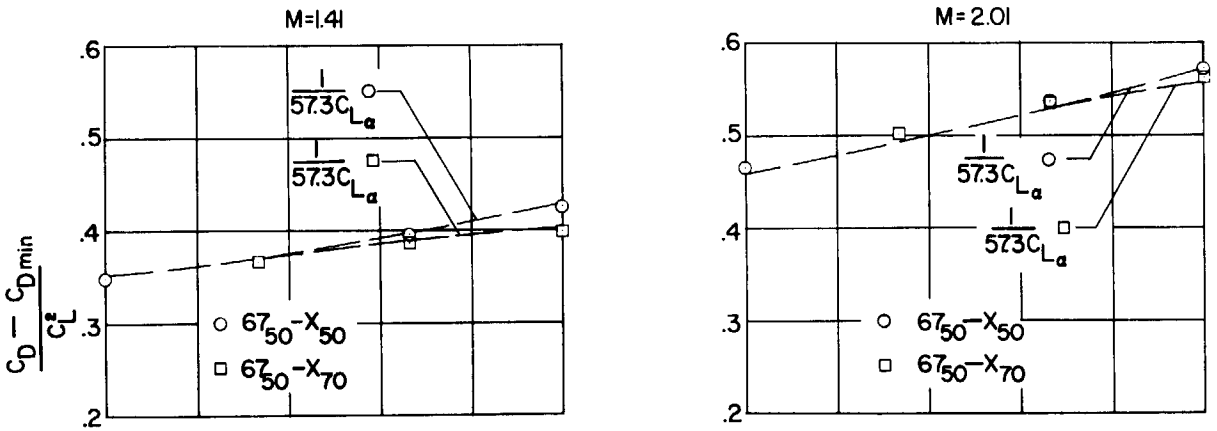

(c) Coefficients based on respective wing areas. Configurations 67_{50}-X_{50} and 67_{50}-X_{70}.

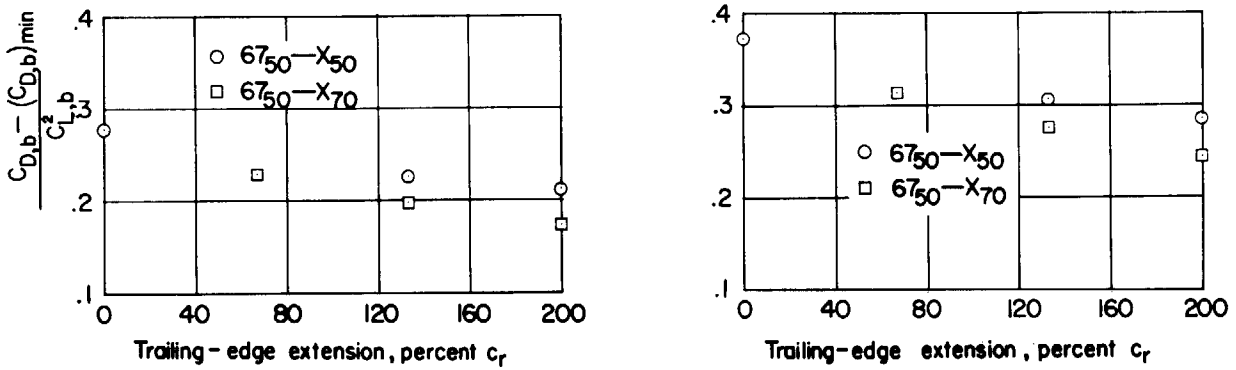

(d) Coefficients based on the area of the basic cranked wing. Configurations 67_{50}-X_{50} and 67_{50}-X_{70}.

Figure 13.- Concluded.

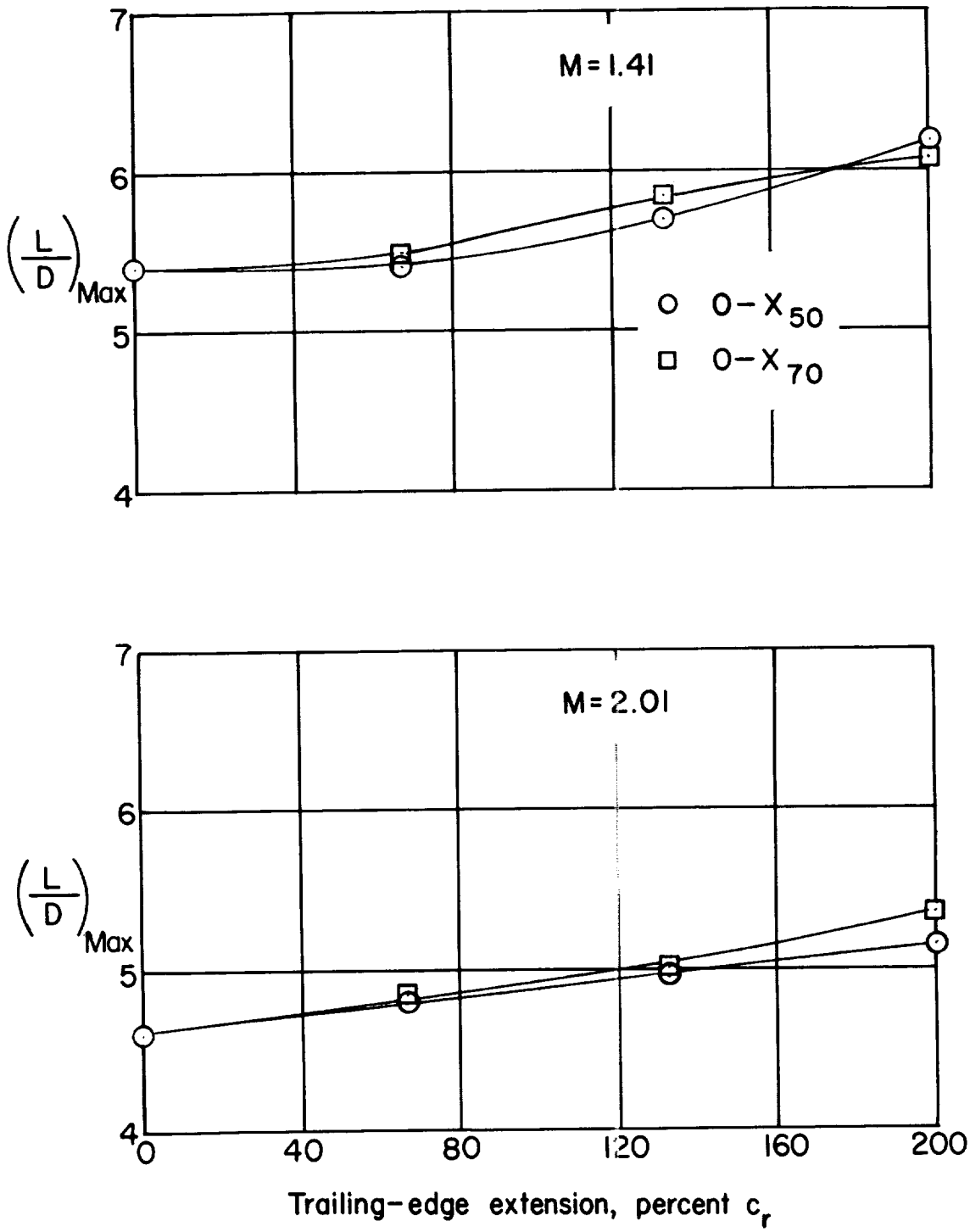

Figure 14.- Maximum lift-drag ratios for the configurations tested.

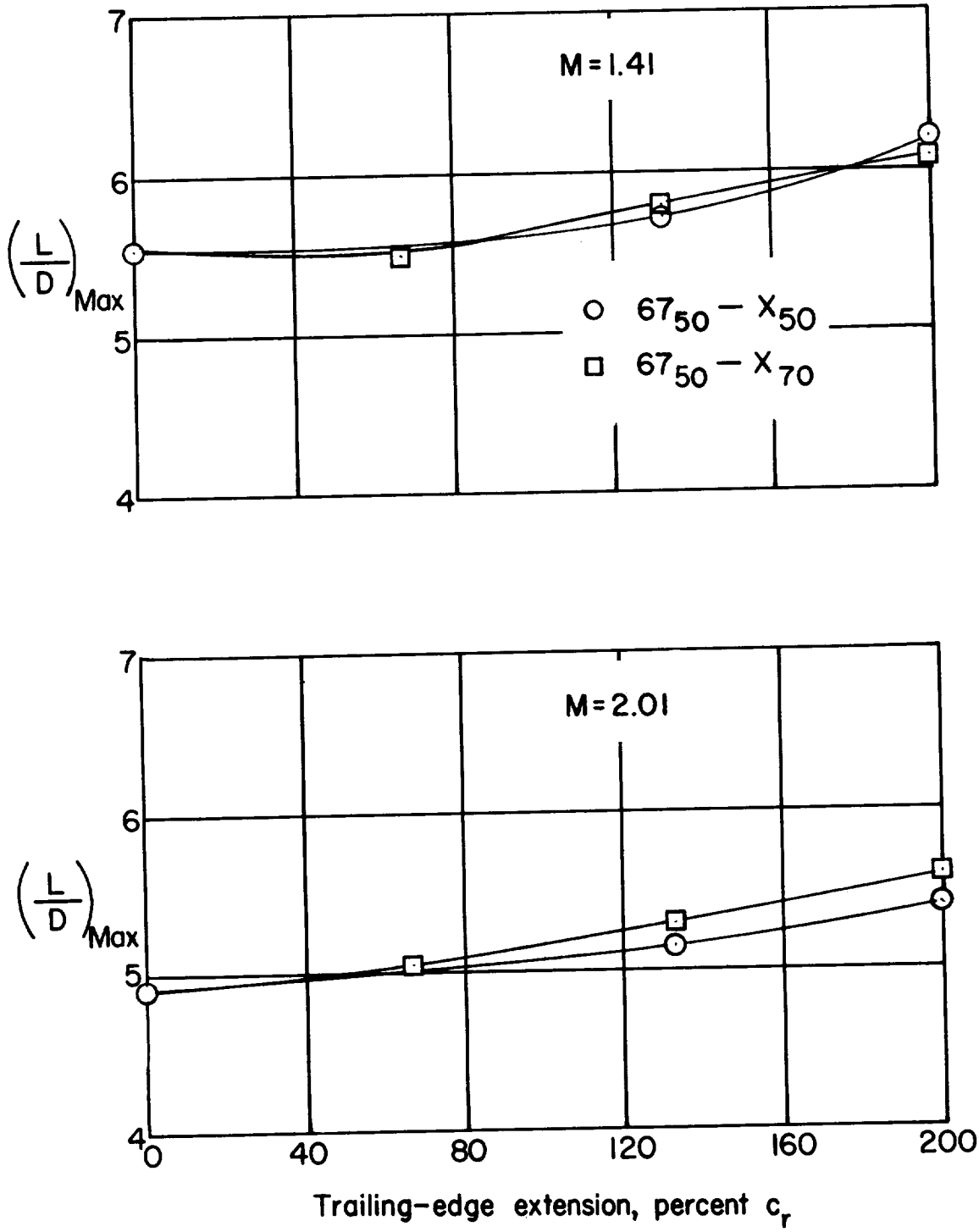

Figure 14.- Concluded.